

Villanova University
The Graduate School
Department of Civil and Environmental Engineering

A Soil Profile Characterization of a Bioinfiltration BMP

A Thesis in
Civil Engineering
By
Keisha Isaac-Ricketts

Submitted in partial fulfillment
of the requirements
For the degree of

Masters of Science in Civil Engineering

August 2008

A Soil Profile Characterization of a Bioinfiltration BMP

By

Keisha Isaac-Ricketts

August 2008

Robert G. Traver, Ph.D., P.E.
Professor
Department of Civil and Environmental Engineering

Date

Andrea Welker, Ph.D., P.E.
Associate Professor
Department of Civil and Environmental Engineering

Date

Ronald Chadderton, Ph.D., P.E.
Chairman and Professor
Department of Civil and Environmental Engineering

Date

Gary A. Gabriele, Ph.D.
Dean
College of Engineering

Date

A copy of this thesis is available for research purposes at Falvey Memorial Library.

Acknowledgements

A great big thank you to everyone who has been supportive and encouraging along this journey. To my family, friends and colleagues, it was certainly a pleasure and relief to have you around. A special thanks to my husband, mother and aunt who always listened and gave advise when needed. Thank you for putting up with everything and understanding. To my friends and colleagues at Villanova, thanks for welcoming me into the team and working together as well as we did. Erika, Megan, Tom, Erin, Hans, Matt G, Matt M, Jim, Krista and Clay- a big thank you and good luck in your current and future endeavors. You guys taught me a lot and you definitely have a bright future ahead of you! George, Mary Ellen and Linda- Thank you for your assistance and going way beyond. Bill- Thank you for all what you taught me and I certainly learnt more than I expected. Your passion for this work was without doubt an encouragement. Dr. Welker- Thank you for guiding me along the right path when soils just seemed way beyond my knowledge. Hopefully I got it right. Dr. Traver- Thank you for welcoming me into your group and trusting that I would do a good job. I have learnt a lot and hydrology makes more sense than when I first started in the field. I appreciate your time and advice during this time.

Abstract

The ability of water to percolate through any infiltration system is highly dependent on the composition and layout of its soil media. Soil properties and location along a system's profile supports water characteristics such as conductivity and suction. While an array of physical and laboratory experiments exist to calculate soil-water characteristics, grain size distribution analyses remains as the most cost effective and relevant. It describes of the physical attributes such as grain size, content and distribution. This study explored this theory by examining soil properties along the topmost and lower depths of the basin of the Bioinfiltration Traffic Island at Villanova University, constructed in 2001. The chemical composition with respect to soil moisture and organic content was also investigated to evaluate soil-water characteristics.

Variation in the physical and chemical soil composition with respect to organic content and soil moisture existed throughout the soil profile. Organic content and soil moisture levels were highest in the topmost layer of the soil profile. A variety of soil particle sizes were observed in the profile and showed little similarity to made soil added during construction. Fine particle soils were predominant in the lower depths of the 1 foot profile evaluated. However, the degree of change in the soil properties from time of construction in 2001 to its current stage does not influence its current infiltration capacity. The layer of fines at lower depths had similar properties to the original soil prior to the addition of sand soils during construction.

The downward movement of fine soil particles during the infiltration process shows the importance of designing a soil bed capable of maintaining its intended conductivity throughout its lifespan. The addition of sands to create a soil mixture that incorporates more void spaces in a less conductive soil, may not uphold its conductivity over a long period. While pre-treatment features serve to reduce the inflow of soil particles and sediment from the drainage area, other soil-water dynamics occurring along the profile influence the basin's lifelong ability to infiltrate efficiently.

TABLE OF CONTENTS

Chapter One: Introduction	9
1.1 Overview	9
1.2 Stormwater Management.....	11
1.2.1 Best Management Practices (BMPs).....	12
1.3 Site Description and Location	13
1.4 Design and Construction	15
1.4.1 Design Overview	15
1.4.2 Bioinfiltration Basin & Bed.....	17
1.4.3 Monitoring Equipment	19
1.5 Research Objectives	21
Chapter Two: Literature Review	23
2.1 Introduction	23
2.2 Soil Structure & Physical Properties	23
2.2.1 Particle Shape & Size	23
2.2.2 Soil Classification.....	25
2.3 Soil Profile & Its Composition.....	27
2.4 Soil & Water Relationship.....	28
2.4.1 Infiltration and Influencing Soil Factors	28
2.4.2 Hydraulic Conductivity	29
2.4.3 Soil Moisture Content.....	31
2.4.4 Soil Profile Stratification	33
2.5 Hydraulic Conductivity & Grain Size Distribution.....	34
2.5.1 Theory and Relevance	34
2.5.2 Hydraulic Conductivity Empirical Formulas	35
2.5.2.2 Empirical Formula Application	36
2.6 Organic Matter: Total Carbon & Nitrogen in Soil	38
Chapter 3: Methods	41
3.1 Introduction	41
3.2 Soil Sampling	41
3.2.1 Locating Test Locations	41
3.2.2 Sampling Procedure.....	43
3.4 Soil Characterization	46
3.4.1 Particle Size Analysis - Hydrometer Method – ASTM D421, ASTM D422	46
3.4.2 Determining Quantity of Sand.....	52
3.4.3 Particle Size Analysis - Soil Sieve Test - ASTM D421, ASTM D422	54
3.5 Hydraulic Conductivity Analysis	56
3.6 Total Carbon and Nitrogen Combustion Analysis	58
Chapter Four – Results	59
4.1 Introduction	59
4.2 Soil Moisture Content.....	60
4.3 Particle Size Analysis	61

4.3.1	Hydrometer Method Calculations	61
4.3.2	Sieve Method Calculations	63
4.4	Fine Particle Content	65
4.4.1	One Foot Soil Profiles (Test Location S1, S2, S3 & S4) and Sample SED	65
4.4.2	Eight Foot Soil Profile (Test Location O1)	66
4.5	Grain Size Distribution Curves	66
4.5.1	Test Locations - S1, S2, S3, S4	67
4.5.2	Sediment Load – SED	71
4.5.3	Surrounding Berm Samples – B1, B2	71
4.5.4	Eight Foot Soil Profile Sample – O1	74
4.5.5	Original (Construction) Sieve Results	75
4.6	Calculated Hydraulic Conductivity	77
4.7	Total Carbon in Soil Profile and Sediment Load	79
4.8	Total Nitrogen in the Soil Profile and Sediment Load	80
Chapter Five – Discussion		81
5.1	Introduction	81
5.2	Organic Matter Distribution: Carbon and Nitrogen	81
5.3	Fine Content & Soil Distribution – 1ft Profile & 8ft. Profile in Basin	82
5.4	Hydraulic Conductivity – 1 ft and 8 ft Profile in Basin	85
5.5	Original Soil vs. Current Soil Profiles	86
5.5.1	Comparison of Designed Soil Bed & 8 ft. Soil Profile Samples	86
5.5.2	Comparison of Berm Sample & 8 ft. Soil Profile Samples	88
5.6	Possible Sources for Soil Adjustments	90
5.6.1	Sediment Load	90
Chapter 6 – Conclusion		91
6.1	Summary	91
6.2	Design & Maintenance Recommendations	94
6.3	Future Research	96
References		98
APPENDIX A-1.....		A
Site Historical Data		
Construction Photographs		
APPENDIX A-2.....		G
AASHTO Soil Classification Chart		
APPENDIX A-3.....		H
Hydrometer Calculation Factors		

APPENDIX A-4.....	K
Hydrometer Calculations and Data	
Soil Moisture Content Data	
Sieve Calculations and Data	
Combined Distribution Curves	
Original Soil Sample Data and Plot	
Hydraulic Conductivity Calculations and Data	

LIST OF FIGURES

Figure 1-0: Map Showing Location of Site	14
Figure 1-1: Plan of the Bioinfiltration Traffic Island Drainage Area (Heasom et al 2006)	15
Figure 1-2: Excavation of Basin with Addition of 12" Pipe	16
Figure 1-3: Addition of Mixed Soil during Construction.....	18
Figure 1-4: Bioinfiltration Traffic Island in Summer and Winter Months.....	19
Figure 1-5: Detailed Plan of Basin and Location of Instruments	21
Figure 2-0: USDA Soil Classification Triangle (USDA).....	26
Figure 2-2: Schematic Representing a Sample Soil Profile (USDA).....	28
Figure 2.3: Soil Moisture Content of a Homogeneous Profile (Hillel 1998)	32
Figure 3.1: Map of Test Locations	42
Figure 3.2: Test Location Showing Composite Sample	43
Figure 3.3: Depths for Each Test Location.....	44
Figure 3.4: Sample Extraction	45
Figure 3.5: Hydrometer Dimensions	48
Figure 3.6: Hydrometer Jars and Control Jar During Testing	50
Figure 3.7: Collection of Sand Particles on No. 200 Sieve	52
Figure 3.8: Fines and Sand Contents after Wash & Weighing of Sand Contents	54
Figure 4.0: Soil Moisture Content Results	60
Figure 4.1: Hydrometer and Sieve Particle Size Distribution Curve for L7	64
Figure 4.1a: Fine Particle Content for Soil Profile Test Locations S1-S4	65
Figure 4.1b: Fine Particle Content for Soil Profile O1	66
Figure 4.3: Test Location S1: Grain Size Distribution Curve	67
Figure 4.4: Test Location S2: Grain Size Distribution Curve	68
Figure 4.5: Test Location S3: Grain Size Distribution Curve	69
Figure 4.6: Test Location S4: Grain Size Distribution Curve	70
Figure 4.7: Comparison of Test Location Curves	71
Figure 4.8: Test Location SED: Grain Size Distribution Curve.....	72
Figure 4.9: Test Location B1: Grain Size Distribution Curve.....	73
Figure 4.10: Test Location B2: Grain Size Distribution Curve.....	73
Figure 4.12: Sieve Analysis Results of Original Soil during Construction.....	76
Figure 4.13: Plots of B samples and Original Sieve.....	76
Figure 4.14: Hydraulic Conductivity Plots for S1-S4	78
Figure 4.15: Hydraulic Conductivity Plot of O1	79
Figure 4.16: Total Carbon Percent Weight for S1-S4 & SED.....	79
Figure 4.17: Total Nitrogen Percent Weight for S1-S4 & SED	80
Figure 5.0: Comparison of Soil Moisture and TOC for S1-S4 and SED	81
Figure 5.1: Comparison of Soil Moisture and Total N for S1-S4 and SED	82
Figure 5.2: Overall Soil Distribution in Basin S1-S4: High Percent Finer Readings for S1	83

Figure 5.4: Sieve Test Results for O1 vs Early Designed Soil: Percent Passing No. 200.....	87
Figure 5.5: Complete Particle Distribution for B2 vs 8ft Soil Profile.....	89
Figure 5.6: Comparison for Particle Distribution of S2 and SED	90

LIST OF TABLES

Table 1-0: List of Bioinfiltration Vegetation.....	19
Table 2-0: Soil Particle Sizes.....	25
Table 2-1: USCS Group Symbol Representation	27
Table 2-2: Hydraulic Conductivity Empirical Formulas	37
Table 3.0: US Standard Sieve Sizing.....	55
Table 4.2: Sieve Test Calculations for S1 L7.....	64
Table 4.3: Hydraulic Conductivity Calculations	77
Table 5.0: Table Showing Fine Particle Content.....	84
Table 5.1: Tabular Results for Hydraulic Conductivity for S1-S4.....	85
Table 5.2: Tabular Results for Hydraulic Conductivity for O1.....	85
Table 5.3: Original Soil Sieve Results.....	86
Table 5.5: Sieve Results Illustrating Fine Particle Content for S2 & SED	90

Chapter One: Introduction

1.1 Overview

The purpose of this research is to investigate the physical changes in the soil profile of the Villanova University bioinfiltration traffic island and potential influences on the system's infiltration capacity. This study aims to understand the dynamics of the soil composition in an infiltration system and its ability to promote efficient infiltration. Research has shown that several soil associated factors can impede or improve the natural percolation of water in any infiltration system (Hillel 1998). Soil particle size, hydraulic conductivity, moisture content, profile stratification, depth and surface conditions are factors controlling soil infiltration. These factors were studied and analyzed for their overall impact on the infiltration capacity at the Villanova University Bioinfiltration Traffic Island. The site consists of a constructed basin with a soil bed designed to enhance infiltration of inflow volumes. The introduction of a poorly graded sand soil into the soil bed allowed larger pore sizes to exist among the original soil mix, promoting a higher hydraulic conductivity along the soil profile. Total organic content within the soil profile was analyzed for this research. The ageing of the bioinfiltration feature allowed a 1 to 3 inch layer of highly organic soil to cover the surface of the basin. Organic matter within the soil presumably originated from the presence of mulch during its early stages, decaying vegetation and the inflow of organic matter from the drainage area.

The performance and longevity of an infiltration BMP is highly dependent on its efficiency to percolate water through soil in a given design period. To maintain these efficiencies, infiltration features must be designed and constructed with soils capable of allowing water to infiltrate the designated design storms in both wet and dry antecedent conditions. Larger particle size soils, such as sands, allow water to move at a higher rate through the profile compared to soils of smaller sized particles, i.e. clays and silts, thus maintaining a higher hydraulic conductivity. The distribution of

soils within a soil profile affects the way in which water infiltrates. Horizontal soil layers within a profile containing varying soil types define the overall infiltration process. Other factors such as antecedent moisture conditions, soil fractures, vegetation and other changes within the soil profile are all capable of influencing infiltration. The study of soil and its ability to transport water through an infiltration system is a vital to their design, construction and overall management throughout their lifespan.

The most common method of analyzing the soil-water relationship is through hydraulic conductivity analyses that can be conducted in both the laboratory and field. Field tests produce more accurate results because the soil is undisturbed. For the purpose of this research, laboratory grain size distribution analyses were conducted at varying depths to investigate the soil-water relationship of the infiltration feature. Field analyses using infiltrometers to measure hydraulic conductivity are not suitable for this research as it would have greatly disturbed the soil profile. To protect the overall soil profile maintained in the basin, sufficient samples of soil were collected at depths from 0 to 12 inches along the soil profile to reduce disturbance. Sieve and hydrometer analyses were performed in the laboratory to create grain size distribution curves of the soils present along the profile. Using the results of the grain size distribution curve, the Sauerbrei Formula was used to calculate the hydraulic conductivity at each depth along the soil profile. The Sauerbrei Formula is a dimensionally non-homogeneous empirical formula used for the determination of hydraulic conductivity in porous media with fine particles of silt and clay (Kasenow 2002).

Organic content along the soil profile of the basin was measured by analyzing the total carbon content for each sample using the LECO TruSPEC Carbon and Nitrogen Determinator. Total nitrogen values were also determined for each sample, as the results reflect a relationship between total nitrogen and pollutant loading. Samples used for both tests are the same as those used on the soil characterization tests mentioned above. It was important to maintain sample consistency

among tests. The LECO TruSPEC uses small soil samples which are incinerated at high temperatures, which releases gases indicating the total carbon and nitrogen by percent weight.

1.2 Stormwater Management

Changes in land use can dramatically alter the hydrology and downstream water bodies within a watershed. In pre-developed conditions, the natural land allows precipitation to be infiltrated or stored in surface depressions along the soil. Vegetation promotes evapotranspiration, the reduction of runoff rates and filters water within the soil. The end results of development from increased impervious cover or conditions indifferent to its pre-existing conditions will reduce these factors aimed at reducing stormwater runoff volumes and rates. The addition of paved roads, driveways, parking lots as well as other impervious features such as roofs, gutters and sidewalks can be responsible for altering the hydrology of the entire watershed.

Similarly, the downstream waterbodies of an affected watershed can experience dramatic changes because of development. As runoff exits the drainage area at higher volumes and rates, it enters the stream in most cases by way of pipes and paved gutters. The use of these conduits shortens the travel time of runoff entering downstream waterbodies producing higher peak flow rates and velocities compared to natural conditions. In pre-developed conditions, the flow rate and volume of runoff would have been reduced by the roughness and infiltration capacity of vegetated conveyances such as swales and vegetated channels. In addition to higher peaks, streams experience increased volumes that result in flooding or full bank conditions. The frequency of these events ultimately leads to changes in stability and appearance of the stream from high erosion and sedimentation levels. Ecosystems of the stream will also be affected as erosion and sedimentation will disturb and remove habitats. This will also affect the quality of water within the streams as high sedimentation can lead to higher levels of pollutants and sediments. A reduction in infiltration from

the addition of impervious area also affects groundwater recharge and baseflow conditions. With smaller volumes of water infiltrating the surrounding developed area, baseflow levels are reduced which may affect any neighboring wetlands or streams.

Increases in stormwater volumes and rates are not the only result of improper stormwater management in urbanized watersheds. The level of pollutants within the watershed and its tributaries are a factor as well. The disturbance of land during development or the accumulation of material on new impervious cover can release pollutants once runoff is produced. Pollutants such as hydrocarbons, suspended and dissolved solids, nutrients, metals and pathogens can be increased in concentration during and after development. An increase in temperature from impervious areas will also be expected. Development also reduces opportunities for these pollutants to be infiltrated through the soil or filtered through vegetated conveyances, as both serve to pollutants present in the watershed. Water quality can also be adversely affected by changes in the temperature of runoff entering streams. Rainfall entering paved areas will maintain higher temperatures compared to those entering vegetated areas and will travel at higher velocity to a nearby waterbody. The impact of warmer waters entering streams will affect the overall ecosystem, with dissolved oxygen as the most influential factor.

1.2.1 Best Management Practices (BMPs)

In response to the ongoing problems associated with urbanization and its effect on water resources, the Environmental Protection Agency (EPA) introduced technical and financial assistance to states and other jurisdictions to improve or initiate stormwater management practices. The introduction of Phase 2 of NPDES under the Clean Water Act promotes the use of Best Management Practice (BMPs) strategies for new development and retrofit of existing development in urban areas. These strategies aim to reduce runoff volume, peak flow and non point source

pollution mainly through infiltration, detention, evaporation and transpiration practices. Compared to historical stormwater management practices that sought only to redirect runoff volumes through conveyance channels or control peak flow through detention of larger infrequent design storms; BMPs aimed at maintaining runoff onsite by reducing overall volume and discharge of small, more frequent annual storms. Pennsylvania, for example, experiences 85 percent of its annual rainfall in increments of 1 inch or less. Detention facilities designed for 25 to 100 year storms will defeat the purpose of reducing the impact on the stream system, as smaller more frequent storms travel unaffected through basins. Current Pennsylvania policy requires BMPs to be tailored to capture the difference in the two year storm through reuse, evapotranspiration and infiltration (PADEP 2006).

1.3 Site Description and Location

The Villanova University Bioinfiltration Traffic Island is located within the Darby Creek watershed in southeast Pennsylvania. The Traffic Island is one of the six BMPs at the Villanova University Stormwater Best Management Practice Demonstrate and Research Park located throughout the university. (Fig 1-0) The site is a retrofitted traffic island within the parking lot of the university's West Campus dormitory complex. The drainage area for the Traffic Island is approximately 1.2 acres and maintains 54 percent impervious cover. The drainage area of the Traffic Island consists of a gravel volleyball court, an asphalt basketball court, green areas, roadway and parking lots. (Fig 1-1) The disconnected impervious area loading ratio at this site is 10:1.

The pre-developed traffic island consisted of mounded turf grass surrounded by concrete curbing. The immediate drainage area surrounding the basin consisted of stormwater inlets and pipes that intercepted runoff to a downstream dry detention basin which provided no infiltration for the treatment of incoming water. The site was designed on the basis of capturing and infiltrating the first inch of rainfall, thereby supporting the then current Pennsylvania Act 167

stormwater approach. By capturing and infiltrating the first inch of rainfall, the site is capable of reducing the pollutant load, volume and discharge rate of more frequent smaller storms.

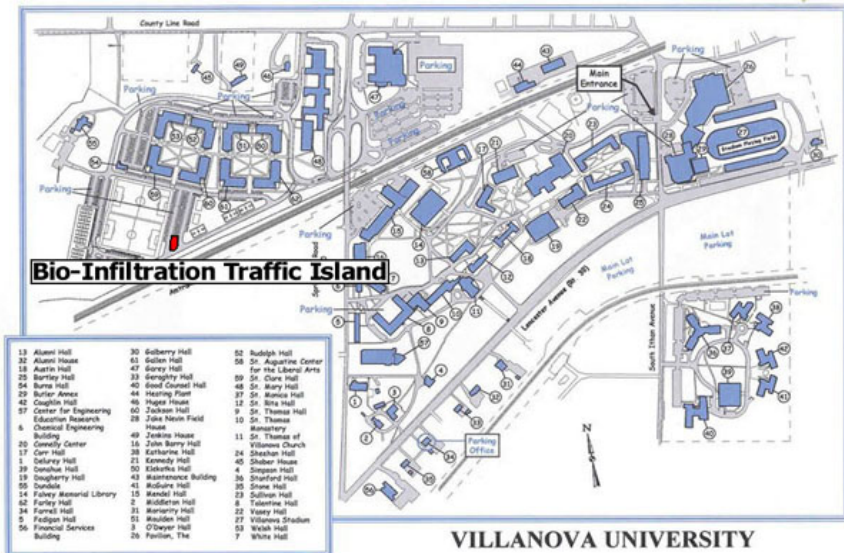


Figure 1-0: Map Showing Location of Site



Figure 1-1: Plan of the Bioinfiltration Traffic Island Drainage Area (Heasom et al 2006)

1.4 Design and Construction

1.4.1 Design Overview

In the summer of 2001, the Bioinfiltration Traffic Island was constructed in the parking lot of West Campus at Villanova University. As part of an award granted by the Pennsylvania Department of Protection (PA DEP) Growing Greener Grant Program, the existing site was designed and retrofitted to capture and infiltrate the first inch of rainfall. The site was designed to allow runoff to be redirected into the basin through a main storm sewer and two curb cuts located in the mains travel paths of incoming flow. A curb cut was created by initially cutting the curb, then filling and paving an existing storm inlet. To identify the travel paths, water was applied in the surrounding drainage area to monitor the areas that received more runoff.

The curb cuts were supported by rip rap channels that served to deliver runoff to the basin protecting the travel path from erosion and sedimentation. The main storm sewer was connected to the basin through a 12 inch corrugated plastic pipe that transported runoff generated from the

roadway (Fig 1-2). To divert water to the basin rather than downstream, a wall was constructed within the inlet. During storms of 1 inch or less, runoff will be directed to the basin through the storm pipe. When the basin exceeds its capacity, water will bypass the diversion and travel downstream to the dry detention basin. To promote infiltration, evaporation and transpiration, the basin is designed and constructed with an infiltrating soil bed and plants tolerable of harsh environments. Additional construction photos are located in Appendix A-1.

During a storm event of 1 inch or more, water enters the basin through its three main conveyances and through direct entry to the surface. The basin gradually fills until it reaches an elevation of 445.93 feet when the water overflows a v-notch weir located in the inlet. At this stage the basin is completely full, vegetation is mostly submerged and water entering from either entrance will be bypassed downstream unless a significant portion is infiltrated. Water will remain in the basin until rainfall ceases, allowing water to infiltrate through the designed soil bed and into the underlying subsoil.



Figure 1-2: Excavation of Basin with Addition of 12" Pipe

1.4.2 Bioinfiltration Basin & Bed

The basin of the bioinfiltration feature was constructed by the excavation of 1907 cubic feet (54 cubic meters) of subsoil in a rectangular shape. A sieve analysis (ASTM D422), Atterberg limits test (ASTM 4318), porosity and soil moisture content test were performed to characterize the native subsoil prior to designing the infiltrating soil bed. The existing subsoil was characterized as a tan, fine grained soil, with little clay content and was classified as ML (silt soil) according to the Unified Soil Classification System (USCS) (ASTM D248) (Heasom 2006). The soil moisture content test was performed on the grassed banks of the basin and was assumed to be that of the native soil. Moisture levels and estimated porosity of the subsoil were 20 and 46 percent, respectively (Prokop 2003).

To improve the porosity and hydraulic conductivity of the existing subsoil; a sandy soil classified as SP (USCS) was mixed with the native soil. This mixture of silt and sand soils was then filled into the excavation to create a 4 foot deep infiltration bed. (Fig 1-3) A survey of the site after construction detailed the volume of the basin at elevation 446.50 feet as 2250 cubic feet. The infiltration bed was estimated to hold a total volume of 4150 cubic feet. In determining the storage capacity of the basin, the porosity of the designed soil bed was estimated at 50 percent therefore reducing storage to 2065 cubic feet. The total storage capacity including the basin's surface volume was summed at 4315 cubic feet (Prokop 2003). To assess the basin's ability to maintain the desired storm requirements of 1 inch, the estimated volume of inflow with the exception of initial abstractions over the 1.2 acre drainage area was calculated at 4221 cubic feet (Prokop 2003). This suggests that the basin was constructed to the design requirements.

To maintain the healthy growth of plants during varying seasons, temperatures and pollutant loads; the chosen plants must be tolerant of these conditions. The plants of the Bioinfiltration Traffic Island are native to the coastal areas of Southern New Jersey. These plants

are capable to withstand extended wet conditions as well as drought conditions. During summer months, plants are in full bloom covering a majority of the surface area of the basin. Grasses grow around the perimeter of the basin, while herbs and woody plants such as berry trees grow within the basin (Table 1-0). Small birds and mammals frequent this area during this time of year. In the fall and winter months most plants to are dormant until the spring (Fig 1-4).



Figure 1-3: Addition of Mixed Soil during Construction

Plant Species	Common Name
Grasses	
<i>Ammophila breviligulata</i>	American Beach Grass
<i>Panicum amarum</i>	Coastal Panic Grass
<i>Panicum virgatum</i>	Switch Grass
<i>Schizachyrium scoparium</i>	Little Bluestem
Herbs	
<i>Solidago sempervirens</i>	Seaside Goldenrod
Woody Plants	
<i>Photinia melanocarpa</i>	Black Chokeberry
<i>Baccharis halimifolia</i>	Groundsel Tree
<i>Ilex verticillata</i>	Winterberry
<i>Iva frutescens</i>	Marsh Elder
<i>Prunus maritima</i>	Beach Plum

Table 1-0: List of Bioinfiltration Vegetation



Figure 1-4: Bioinfiltration Traffic Island in Summer and Winter Months

1.4.3 Monitoring Equipment

The Bioinfiltration Traffic Island site is equipped with water quality and quantity apparatus used for measuring, sampling and monitoring, precipitation, pollutant loading, as well as inflow and outflow volumes (Fig 1-5). Precipitation received at the site is measured using an American Sigma tipping bucket rain gauge which relays data to an American Sigma 950 data logger. All recording instruments on site are connected to the data logger, allowing information to be easily accessible through downloading on the American Sigma DTU II. This downloader transfers downloaded data from any instrument on site to a software capable personal computer. An American Sigma 75 KHz Ultrasonic Transducer (Model 1176-01) is installed on site for recording water surface elevations in the basin. The instrument is calibrated with a staff gauge mounted on the transducer allowing users to read off the water surface elevation values. Outflow to the downstream conveyance system is estimated using a 90 degree v-notch weir and a newly

installed pressure transducer. Both instruments are located in the main storm inlet. The addition of the pressure transducer allows more accurate depth recordings of water exiting the site during larger storms.

Water quality is monitored by the use of first flush samplers and suction lysimeters. First flush samplers are used to sample and measure runoff pollutant loads during the initial stages of a storm event. There are two first flush samplers located on site; each is located above both rip rap channels leading the basin. Each sampler houses a rectangular plastic container which is removed once the sample is acquired. There are three suction lysimeters located in the soil bed and subsoil of the basin. These instruments are capable of extracting water samples at various depths along the soil profile. The lysimeters are located at the near the surface, as well as 4 and 8 feet below the surface of the basin. The site also maintains three soil moisture meters connected to the data logger, located at 2, 4 and 8 feet below the surface. There are two wells located in the surrounding grass area above the basin. Both wells extend to depths beyond the four foot soil bed and are equipped with pressure transducers for measuring the water depths.

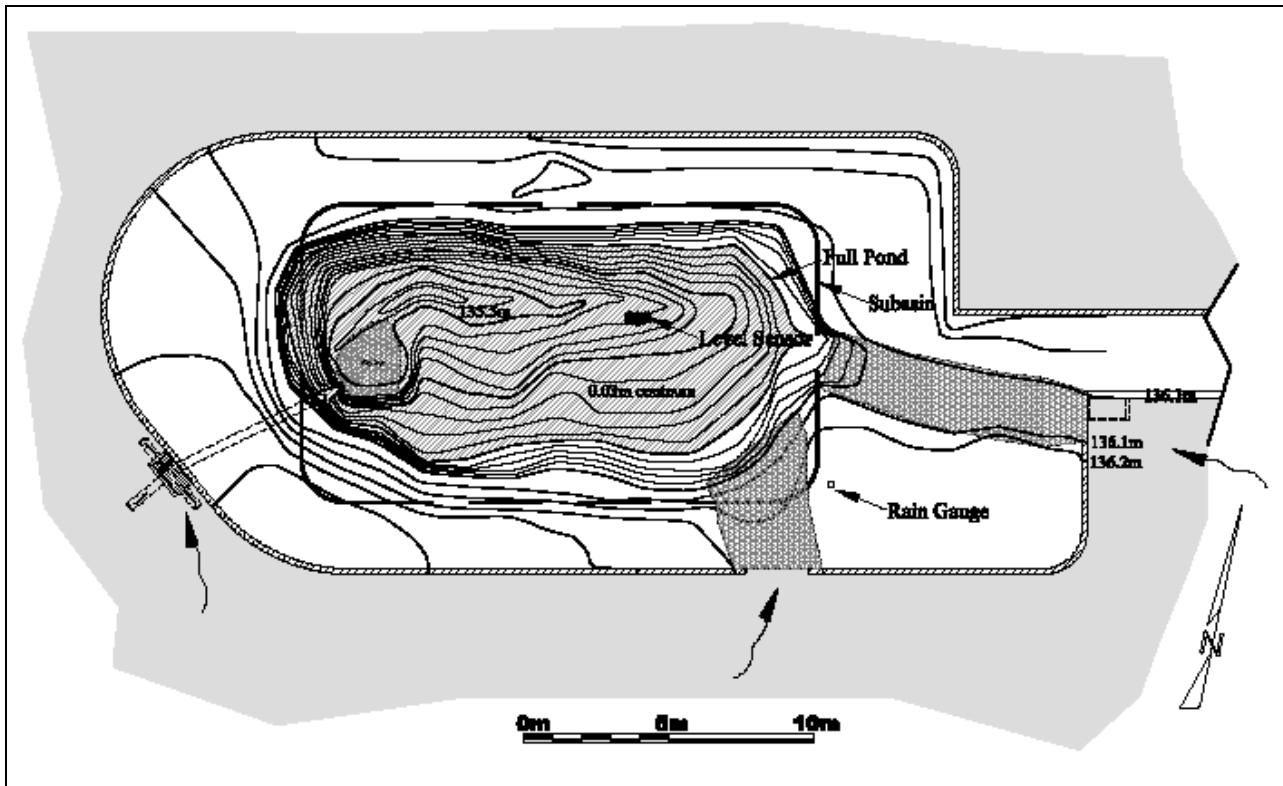


Figure 1-5: Detailed Plan of Basin and Location of Instruments (Heasom 2006)

1.5 Research Objectives

Steps to meet the objectives of this research were as follows:

- (1) *Characterize and identify the soil particles (sands, clays and silts) present within the basin of the Traffic Island.* Soil particles were identified at various locations along the basin that each reflected a composite distribution in a given area. At each location, soil types were identified at various depths along the soil profile. In addition, each soil type was quantified at each location and depth to develop ratios of each soil type in a given sample. This step established the possibilities of any stratified layers or areas of drastic unequal distribution of the silt and sand mixture, as it would relate the mass of each soil type at a given horizontal location and depth.
- (2) *Study organic carbon with respect to its distribution in the soil profile.* This objective

identified the influence of highly organic soils in the basin of the Bioinfiltration Traffic Island. The percent weight of total organic carbon in each location and at each depth along the profile was performed. Although organic matter is most prevalent in the topmost layer of the basin, early stages of research has shown low levels of organic matter in depths below the surface. It was also important to investigate the distribution of organics within the basin as it may influence water quality. Analysis of organic carbon was conducted on the LECO CN Determinator.

(3) *Study total nitrogen with respect to its distribution in the soil profile.* Total nitrogen was analyzed using the LECO CN Determinator, similar to the organic content analysis. This objective quantified the soil's ability to absorb nutrients such as nitrogen, as water infiltrates through the soil profile. Nitrogen is a prominent nutrient in stormwater runoff. The results of this research gave better understanding of soil and water quality improvement with respect to total nitrogen. By analyzing soil samples on the LECO machine, the distribution of nitrogen along both horizontal and vertical locations was be produced.

(4) *Compare and contrast the original soil characterization with the current soil distribution.* During construction of the site, a soil sieve analysis was performed to classify the soils. A percolation test was also conducted to measure the rate at which water infiltrated the designed soil bed. After five years of existence, this research explored a complete soil characterization to investigate any changes or similarities in the soil profile and compare the hydraulic conductivities of both soils was performed. Hydraulic conductivity, soil particle size distribution with respect to location within the soil profile was emphasized in this comparison.

(5) *Investigate the cause of any changes in the soil profile.* If data showed significant changes in the soil profile from its original stages; the causes, or sources of this adjustment will be identified and explained. This information aids in understanding the dynamics of the surrounding drainage area and the soil profile of the basin. Conclusions from this research can contribute towards the

theory behind sediment loading ratios and the contributing stormwater feature.

Chapter Two: Literature Review

2.1 Introduction

This section reviews various theoretical analyses and research studies on soil grain distribution and hydraulic conductivity. Other soil characteristics such total carbon and nitrogen storage and its relationship with water quality will be discussed in this chapter.

2.2 Soil Structure & Physical Properties

Soil can be defined as the weathered outer layer of the earth's terrestrial surface. It is formed initially through disintegration and decomposition of rocks by physical and chemical processes, and is influenced by the activity and accumulated residues of numerous microscopic and macroscopic plants and animals (Hillel 1998). Soil does not exist naturally as a homogeneous body, but is composed of varying soil types, minerals and levels of organic matter at different depths.

Soil can simultaneously contain solid, liquid and gas phases. The liquid and gas phases are contained in the pore spaces between soil particles. Soil particles represent the solid phase and consists of particles derived from rock. Organic matter can also be included in the solid phase of soil. The liquid phase represents water and other liquid materials capable of leaching into the soil. When the liquid phase does not completely fill pore spaces, the gas phase occupies the remaining pore space. The gas phase can represent naturally occurring gases in the environment as well as vapors produced from pollutants present in the soil. These three phases often interact and usually determine the overall behavior and characteristics of the soil.

2.2.1 Particle Shape & Size

Soils can be divided into three groups: silts, clays and sands. Each particle, or grain, has varying size and shape characteristics that can influence the overall infiltration properties of a soil profile. Silt and clay particles are finer grained, while sands are coarser. The shape of soil particles can be described as: bulky or equidimensional grains, flaky or plate-like grains, and elongated grains and fibers (Winegardner 1995). Bulky or equidimensional grains may be very angular, angular, subangular, subrounded, rounded, and well rounded. Sand and silt particles are bulky, while clay particles are as plate-like which creates a much larger surface area to mass ratio than other soil particles. This ratio known as the specific surface serves to provide contact area between particles and more area for water molecules to attach to soil particles. This characteristic allows clay particles to maintain a greater affinity for absorbing water.

According to ASTM standards (D2487), particles greater than 3 inches in diameter are known as rock fragments (Coduto 1999). Smaller particles are categorized as soil, and are further classified according to their individual grain size (Table 2-0). Sieve and hydrometer analyses are commonly used to classify soil particles through their soil particle size distribution. Larger soil particles are classified using a sieve analysis, whereby soil particles are strained through a series of wire meshes with varying opening sizes. The hydrometer analysis specifies the distribution of smaller particles by measuring a series of specific gravities and applying Stoke's Law. The Methods Section will further detail each analysis.

Particle Dia. (mm)	Soil Classification
> 350	Boulder
75-350	Cobble
19-75	Coarse Gravel
4.75-19	Fine Gravel
2-4.75	Coarse Sand
0.425-2	Medium Sand
0.075-0.425	Fine Sand
< 0.075	Fines (Silt & Clay)

Table 2-0: Soil Particle Sizes

2.2.2 Soil Classification

Soil particle characteristics are better understood and illustrated using soil classification systems. Several soil classification systems use grain size distribution and Atterberg limits to classify these systems are often supplemented by non standardized classification of other properties such as consistency and cementation (Coduto 1999). There are three common soil classification systems: United States Soil Department of Agriculture Soil Classification System, American Association of State Highway and Transportation Organization Soil Classification System, and the Unified Soil Classification System.

The USDA Soil Classification System is a textural soil classification system and is used in many soil survey reports and agricultural research. Soil sizes for USDA are as follows: coarse fragments: >2.0mm, sand: 0.05-2.0 mm, silt: 0.002-0.05 mm and clay: < 0.002 mm. Using the total percent weight of sand, silt and clay particles individually in a given soil sample, the soil can be classified using the USDA soil classification triangle (Figure 2-0). This triangle does not take into account the percent weight of rock fragments that may be present in the soil sample. There are three sets of lines in this triangle, each representing a soil particle. The percent weight of clay is represented by a series of horizontal lines. Silt is characterized by lines inclined from

the upper right to the lower left and sand particles by lines inclined to the lower right to upper left.

The AASHTO System was created for use in highway construction, but is used in a wide array of projects. This system uses both grain size distribution and Atterberg limits data to assign group classification and a group index to a soil. The group index ranges from A-1 to A-8; which represents both the high quality and low quality soils. Group index values near 0 indicate high quality soils, and values nearest to 20 represent low quality soils. The system does account for particles equal to or less than 3 inches in diameter. Figure 2-1 illustrates the system chart used to classify soils.

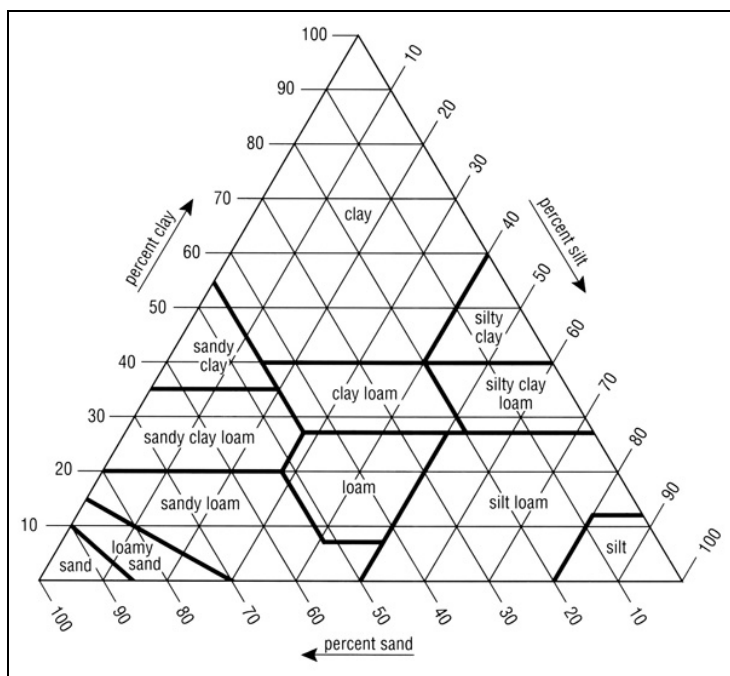


Figure 2-0: USDA Soil Classification Triangle (USDA)

The Unified Soil Classification System (USCS) is unlike the AASHTO System as it can be used to classify soils for varying projects and purposes. The original form of this system consisted of two or four letter group symbols. The system was later changed to include group names to the corresponding group symbols. The initial soil classification of the existing soil at

the site was determined as group symbol “ML” and group name “silt soil” using the USCS system (Heasom 2006), (Prokop 2003). For fine grained soils such as the existing soil at the Bioinfiltration Traffic Island, the first and second letters of the group symbols represent the predominant soil by percent weight and the level of plasticity, respectively. (Table 2-1) This can also be seen for coarser grained soils such as sands and gravel that maintain less than 50 percent passing through the No. 200 sieve. The group names for both grained soils are positioned to represent the percent weight content of each soil grain in a given sample. The noun reflects the predominant component while the adjective reflects the secondary component. A tertiary component can then be used to identify an additional soil type (Coduto 1999). For example: a soil sample with 75% sand, 20% clay and 5% gravel is labeled as clayey sand with gravel.

Fine-Grained Soils			
First Letter	Soil	Second Letter	Soil
M	Predominantly silt	L	Low plasticity
C	Predominantly clay	H	High plasticity
O	Organic		
Coarse-grained Soils			
First Letter	Soil	Second Letter	Soil
S	Predominantly sand	P	Poorly graded
G	Predominantly gravel	W	Well graded
		M	Silty
		C	Clayey

Table 2-1: USCS Group Symbol Representation (Coduto 1999)

2.3 Soil Profile & Its Composition

The characteristics of a soil and its ability to interact with other soil depend on its entire depth or soil profile. From a soil scientist’s view, a soil profile typically consists of three general soil layers or horizons, O, A, B and C. The O horizon is solely organic matter. This layer is composed of decomposing plant and animal matter, as well as other organic litter. The topmost soil layer, or A horizon is typically rich in organic matter as it maintains most of biological

activity in the soil profile. The soil in the A horizon is dark in color compared to soils beneath, and hosts diverse ecological processes because of the presence of plants and animals on the surface. The B horizon is a much denser layer compared to the A horizon as it typically tends to store accumulated fine soil particles that have leached from the A horizon during infiltration.

The accumulation of fine soil particles and the pressure of the overlying soil combine to reduce the porosity of the deeper layers. An overly dense B horizon may inhibit aeration, internal drainage of water and the penetration of roots (Hillel 1998). The C horizon consists mainly of weathered and fragmented rock material. In some cases, the C horizon may consist of the soil's parent material. Each horizon can further be divided into layers to represent varying characteristics within each horizon. Beneath the C horizon lies consolidated rock or bedrock (Fig 2-2). Note that the depth of each horizon can vary from those illustrated in Fig 2-2.

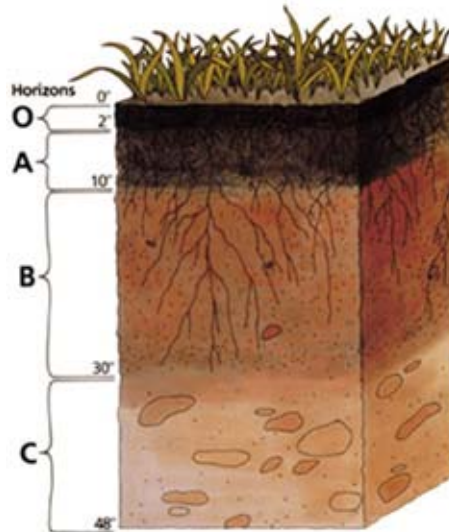


Figure 2-2: Schematic Representing a Sample Soil Profile (USDA)

2.4 Soil & Water Relationship

2.4.1 Infiltration and Influencing Soil Factors

Infiltration is typically defined as the downward movement of water and other solutions through soil. Infiltrated water reenters the water cycle through evapotranspiration and entrance into the groundwater. The rate at which infiltration occurs initially depends upon the amount of water or solution applied to the soil surface. However there are several factors that can influence or impede the flow of water into soil. An important influencing factor is the soil surface conditions, as this area controls the initial entry of water into the soil profile. The soil surface is controlled by several factors such as soil type and texture, the presence of vegetation and compaction. Surfaces comprised of either coarse or fine grained soils can be greatly influenced by compaction during or after construction. However, research has shown that sandy soils tend to be more impacted by compaction (Pitt et al. 1999).

Compaction causes pore spaces to be reduced, decreasing conductivity and sorption. The surface may also have a crusted layer that is less permeable than the soil profile beneath. This crusted top layer is developed when a bare surface area experiences constant rainfall or flooding creating a thin, semi sealed layer (Hillel 1998). Other factors impacting the overall infiltration through the soil profile include the hydraulic conductivity of soils, soil moisture content, and stratification.

2.4.2 Hydraulic Conductivity

Hydraulic conductivity (K) is defined as the rate at which a geologic material, such as soil, can transmit or conduct water under a hydraulic gradient, or the change in head, over the distance of two points. Like other aquifer properties, such as transmissivity and storativity; high hydraulic conductivity is considered crucial for successful groundwater development and management practices (Alyamani and Sen 1993). Hydraulic conductivity is dependent on the diameter, texture and shape of pore spaces through which the water flows.

Soils with large pore spaces are better conductors of groundwater flow compared to soils of small, tightly closed pores, such as clay and some silt. Grain size and shape allow coarse grained soils, such as sand and gravel, to conduct or transmit at higher hydraulic conductivities. The soil properties of fine grained soils restrict higher conductivities. Hydraulic conductivity is dependent on the liquid properties of the infiltrating substance. Density and viscosity of this liquid will alter the hydraulic conductivity.

Darcy's experimental studies of flow through porous soil led to the development of the Darcy Equation. (Kasenow 2002)

$$K = \frac{QL}{\omega \Delta H} = \frac{Q}{\omega J} \quad (\text{Eq 2-1})$$

where

L = distance between which ΔH is measured = (L)

ΔH = head loss = (L)

Q = flow = (L^3/T)

K = hydraulic conductivity = (L/T)

J = hydraulic gradient = $\frac{\Delta H}{L}$

ω = cross-sectional area of the flow

Vukovic and Soro (1992) suggest there are two methods for determining hydraulic conductivity: direct and indirect. Direct measures of hydraulic conductivity are through laboratory and field experiments. Indirect measures are through the use of grain size distribution empirical formulas and the use of mathematical models to represent the physical soil

characteristics. There are several types of laboratory and in-situ tests for measuring hydraulic conductivity. Although both laboratory and in-situ methods are used, there is skepticism on the use of either depending on the type of work being investigated (Coduto 1999). Laboratory tests may not be as accurate as in-situ tests used to investigate K (hydraulic conductivity) is most likely disturbed because laboratory tests such as constant head and falling head, can, however produce estimates that may be helpful. Some in-situ methods for measuring hydraulic conductivity are as follows: Guelph permeameter, velocity permeameter, disk permeameter, slug test, pumping test and double and single ring infiltrometer tests (Mohanty et al. 1994). Grain size can be used to estimate hydraulic conductivity. This method uses the physical soil properties of a given sample and empirical analyses to determine hydraulic conductivity. For the purpose of this research, this method for measuring hydraulic conductivity will be used. The theory of this method and relating analyses are discussed in Section 2.5.

2.4.3 Soil Moisture Content

Bodman and Colman (1965) observed that moisture distribution in soil occurred during vertical infiltration when ponding occurs at the surface. An infiltration soil moisture profile consists of saturation, top transmission, transmission and wetting zones, and wetting front (Bodman and Colman 1965) (Fig 2.3). Under unsaturated conditions, these zones are fairly constant in moisture levels. When ponding occurs the surface area becomes saturated for the first few centimeters in depth, while the remaining depths are dry, or less saturated. Beneath this saturated zone lies the top transmission zone which is less saturated and slightly longer in depth than the saturated zone above. The transmission zone is located directly beneath the top transmission zone and is much longer in depth than both zones above. At this point, the moisture content has significantly decreased from the saturated zone and now maintains a more constant

rate throughout this zone. The wetting zone however maintains a much more rapid change in moisture content that increases with time. The transition into the wetting front from the wetting zone allows a steep moisture gradient to exist between the two areas. The wetting front is significantly different from the wetting zone as it is usually less saturated than the top zone.

In terms of water, or moisture content, soil can exist in both unsaturated and saturated states. An unsaturated soil maintains some pore space filled with air in the presence of water within the soil profile. Water flow in an unsaturated soil may occur either as film creep along the walls of wide pores, or as tube flow through narrow water filled pores (Hillel 1998). The movement of ponded water through an unsaturated soil profile is controlled by a higher suction head at lower, less moist depths. Water will move from water filled pore spaces to air filled pores below. A saturated soil profile maintains water filled pore spaces throughout the soil profile. A fully saturated soil profile usually occurs in the latter stages of ponding or in complete infiltration. Water flow in a saturated soil profile is in the direction of decreasing total head. Throughout a saturated profile the hydraulic conductivity is fairly constant and is reflective of the soil texture and grain size. The order of magnitude is about 10^{-4} to 10^{-5} m/sec for sandy soils and 10^{-6} to 10^{-9} m/sec for clayey soils (Hillel 1998).

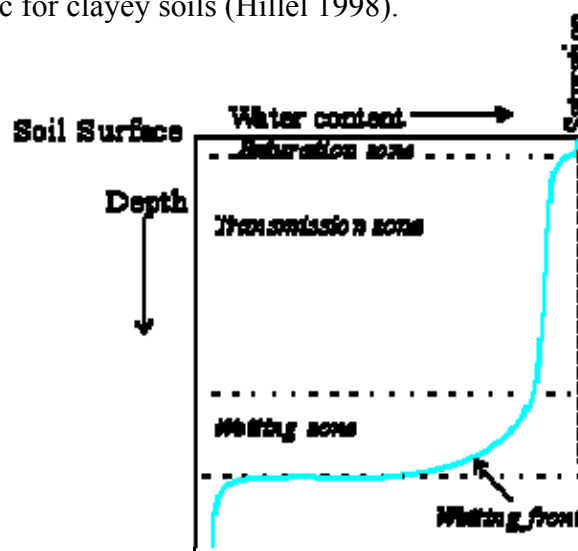


Figure 2.3 – Soil Moisture Content of a Homogeneous Profile (Hillel 1998)

2.4.4 Soil Profile Stratification

As described in Section 2.2, the natural state of a soil profile exists with varied horizontal or vertical layers of soil stratification, rather than in a homogeneous state. In some cases, extreme stratification may cause varying sized grains and textures to exist within close proximity of each other. This causes variability to exist along the soil profile in terms of hydraulic conductivity and soil moisture content, allowing the overall infiltration capacity to differ than in soils with a more uniform soil distribution. The solution of the flow equation for such conditions is apparently impossible by analytical means, and hence, progress in the development of more realistic theories of infiltration has suffered (Hillel 1998). Contrary to most infiltration research that ignores the presence of heterogeneity along the soil profile, some researchers have shown that infiltration is impeded by soil profile variation.

Miller and Gardener (1962) conducted experiments showing the effects of thin soil layers in between uniform soils of equaling grain size and texture. Their results showed that while suction and hydraulic head must remain continuous throughout the profile regardless of stratification, hydraulic conductivity and soil moisture content reflected variability along the soil layers (Miller and Gardener 1962) and (Hillel 1998). Regardless of depth along the soil profile, soil layers can impede the entry of water from one layer into the other. This intrusion is caused by the interface that exists between both soil layers. As water exits a more conducting soil layer and enters a less conductive layer, the change in soil grains, pore sizes and moisture levels interrupt the its flow rate. If infiltration continues over a long period, a perched water table may develop in the top layer, right above the interface. A perched layer will also exist if a less conductive, fine grained soil layer lies above a less conductive, coarse soil layer (Hillel 1998).

Smith (1990) conducted research on two layer soil profiles specifically studying the relationship of the crusted layer to the layer beneath. His work showed that the less permeable

layer controlled the rate at which ponding occurred at the surface compared to profiles without a crusted layer. The physical properties such as the high bulk density and narrow pores of the crusted top layer lead to a much lower hydraulic conductivity compared to the soil beneath. Several researchers previous to Smith, considered this phenomenon analytically. Edwards and Larson (1970) adapted Hanks and Bowers (1962) numerical solution, showing that an overall exponential decrease in saturated conductivity for soil profiles with a crusted top layer. Stratification studies prove that the layer of lower conductivity controls the overall infiltration process of the soil profile.

2.5 Hydraulic Conductivity & Grain Size Distribution

2.5.1 Theory and Relevance

Grain size distribution analysis as mentioned previously, is one way to determine hydraulic conductivity of soil a sample. The main advantage of this method is that it is efficient and inexpensive when compared to most laboratory and field experiments. However, the limitations of this method are its ability to study a fully undisturbed sample of soil that may contain burrows and air spaces that may aid infiltration. Although, the use of empirical formulas can be questionable; there is a physical relationship between grain size and hydraulic conductivity. Since hydraulic conductivity is the measure of the ease with which fluid flows through porous material, certain relationships are expected to exist between hydraulic conductivity and statistical parameter that describe the grain size distribution of a soil medium (Alyamani and Sen 1993).

Grain size distribution analyses produce curves that detail the fractions of soil grains within a soil sample. To produce a distribution curve mechanical analyses, both sieve and hydrometer tests, are conducted to determine the grain size distribution, which is usually

presented in graphical form. Sieve analysis is used for larger sized particles and the hydrometer is used to determine the distribution of silts and clays. Chapter 3 further describes the theory and procedures of both mechanical analyses. The effective grain diameter, d_e , obtained from the distribution curve can be used to represent the relationship between hydraulic conductivity and grain size distribution (Vukovic and Soro 1992). This represents the spherical grain diameter of a uniform porous medium with the same hydraulic conductivity as the corresponding soil sample.

. Effective grain diameters can be defined $d_e = 10, 17$ or 20 percent finer, where the corresponding values denote the percent passing. Hydraulic conductivity is proportional to the square of d_e (Vukovic and Soro 1992).

2.5.2 Hydraulic Conductivity Empirical Formulas

Several empirical formulas exist to characterize grain size distribution as a function of hydraulic conductivity. These empirical formulas are often used to determine the hydraulic conductivity of a porous soil, but are commonly used out of context. The proper use of empirical formulas requires conditions similar to how they were developed. Early research of these formulas sought only to describe porous soil as uniform sized coarse grained soil with little or no trace of fine soils. Also, many researchers failed to detail and state the applicability of these equations when solving for hydraulic conductivity in published documents (Kasenow 2002). Studies have since evolved to determine the applicability of several empirical formulas when characterizing various textured porous soil. Vukovic and Soro (1992) and Kasenow (2002) investigated eleven empirical formulas to determine their domains of applicability with respect to the content of a porous soil. Several models to interpret this relationship have also been developed. Fredlund et al. (1997) and Alyamani and Sen (1993) created models using varying empirical formulas to estimate hydraulic conductivity using soil data. Skaggs, Arya et al. (2001)

went further by creating a model for determining hydraulic conductivity with limited grain size distribution data for both coarse and fine soils.

$$K = \frac{g}{\nu} \cdot \beta \cdot \vartheta(n) \cdot d_e^2 \quad (\text{Vukovic and Soro 1992) and (Kasenow 2002}) \quad \text{Eq 2-3}$$

where

K = hydraulic conductivity = (L/T)

g = gravitational constant = 9.81 (L/T²)

ν = kinematic coefficient of water viscosity (L/T)

$\vartheta(n)$ = porosity function

β = dimensionless coefficient

d_e = effective grain diameter of porous media (L)

2.5.2.2 Empirical Formula Application

Formulas were considered by Vukovic and Soro (1992) and Kasenow (2002) for their applicability to various porous soils. Formulas by Beyer, Hazen, Kozeny, Sauerbrei, USBR, Pavchich, Slichter, Kruger, Terzaghi, Zamarin and Zunker were investigated in depth in Table 2-2. From this analysis, the Sauerbrei Formula was found to be the most suitable for the characteristics of the existing soil and basin soil profile. The domain of applicability is for porous soils with fine soil content such as clay and silt grains. The Sauerbrei formula is expressed as Equation 2-7. This formula uses an effective grain size diameter of 17, meaning the reflective diameter equates to a percent passing of 17 percent.

Author	Value of β	Function of Porosity	Effective Grain Dia.	Domain of Applicability
Beyer	$6 \times 10^{-4} \log (500/C)$	1	$d_e = d_{10}$	$0.06 \text{ mm} < d_e < 0.6 \text{ mm}$
Hazen	6×10^{-4}	$[1 + 10(n - 0.26)]$	$d_e = d_{10}$	$0.1 \text{ mm} < d_e < 3 \text{ mm}$
Kozeny	8.3×10^{-4}	$n^3 / (1-n)^2$	$d_e = d_{10}$	large grained soils
Sauberei	3.75×10^{-4}	$n^3 / (1-n)^2$	$d_e = d_{17}$	sand and sandy clay soils
USBR	4.8×10^{-4}	1	$d_e = d_{20}$	Medium grained soils
Pavchich	1	$n^3 / (1-n)^2$	$d_e = d_{17}$	$0.06 \text{ mm} < d_e < 1.5 \text{ mm}$
Slichter	0.01	$n^{3.287}$	$d_e = d_{10}$	$0.01 \text{ mm} < d_e < 5 \text{ mm}$
Kruger	4.35×10^{-5}	$n / (1-n)^2$	Eq 2-4	Medium grained soils
Terzaghi	$10.7 \times 10^{-3} > \beta T$	$(n-0.13)/(3\sqrt{1-n})^2$	$d_e = d_{10}$	large grained soils
Zamarin	8.3×10^{-3}	$n^3 / (1-n)^2$	Eq 2-5	large grained soils
Zunker	$0.7 \times 10^{-4} > \beta z > 2.4 \times 10^{-3}$	$[n / (1-n)]^2$	Eq 2-6	fine-medium grained soils

Table 2-2 Hydraulic Conductivity Empirical Formulas (Vukovic and Soro

1992),(Kasenow 2002)

$$\frac{1}{d_e} = \sum_{i=1}^{i=n} \frac{\Delta g_i}{d_i} = \sum_{i=1}^{i=n} \Delta g_i \left[\frac{2}{d_i^g - d_i^d} \right] \quad (\text{Kasenow 2002}) \quad \text{Eq. 2-4}$$

$$\frac{1}{d_e} = \frac{3}{2} \frac{\Delta g_1}{d_1} + \sum_{i=2}^{i=n} \Delta g_i \left[\frac{\ln \frac{d_i^g}{d_i^d}}{d_i^g - d_i^d} \right] \quad (\text{Kasenow 2002}) \quad \text{Eq. 2-5}$$

$$\frac{1}{d_e} = \frac{3}{2} \frac{\Delta g_1}{d_1} + \sum_{i=2}^{i=n} \Delta g_i \frac{d_i^g - d_i^d}{(d_i^g)(d_i^d) \ln \left(\frac{d_i^g}{d_i^d} \right)} \quad (\text{Kasenow 2002}) \quad \text{Eq. 2-6}$$

where

Δg_i = weight content of certain fractions of the material composition

d_i = arithmetic mean grain diameter of the corresponding fraction

d_i^s = max. grain diameter of the corresponding fraction

d_i^d = min. grain diameter of the fraction

$$K = 3.49 \left[\frac{n^3}{(1-n)^2} \right] \pi d_{17}^2 \quad \text{Eq. 2.7}$$

where

K = hydraulic conductivity (L/T)

n = porosity

τ = correction for temperature

d_{17} = effective grain size diameter (L)

2.6 Organic Matter: Total Carbon & Nitrogen in Soil

Soil organic matter is a complex mixture ranging from decomposed plant and animal remains to complex polymeric humic materials arising from microbial or chemical degradation processes (Morrill et al. 1982). An organic substance entering the soil ecosystem faces three ultimate fates: (1) it may be totally mineralized and thereby returned to the carbon dioxide and mineral nutrient pool; (2) it may be assimilated into microbial biomass; or (3) the organic matter may be incorporated either unchanged or partially modified into the more stable soil humic fraction (Tate 1987). For the purposes of this research we shall study the latter fates of the entrance of organics. The source of the site's organic matter is contained within decomposed

plant and animal material and the possible organic substances entering the basin from the drainage area. Soils with high organic content tend to be darker and coarse in texture compared to soil grains. Soils subjected to long ponding periods generally accumulate greater concentrations of organic matter than do arable soils (Tate 1987).

The presence of organic matter has physical, chemical and biological benefits in the soil profile. A high organic matter presence increases the cation exchange capacity in soil. With the addition of negatively charged clay particles and organic matter, the level of cation exchange capacity increases. This physical benefit as well, as others, allows organic soils to have potent adsorption capabilities. Organic pollutants such as nutrients and some pesticides entering the soil are reduced by the presence of organic matter and allow lower biodecomposition rates. These pollutants interact with the organic carbon through mechanisms such as ionic attractions, van der Waals forces and covalent bonding. Tate (1987) found that soil organic matter can affect infiltration, soil moisture content as well as evapotranspiration from the soil surface. In a study by Simka (1983) found that evapotranspiration which is controlled by the temperature of the soil surface, can be influenced by the presence of organic matter contained in the soil. Stevenson (1982) suggests that the higher the organic content, the greater the soil's water retention capability. The biological benefit of organic matter in soil supports its needs for nutrients such as nitrogen, phosphorous and sulfur. The properties of soil organic matter allow these nutrients to be retained in the soil at depths closest to the surface to support plant growth.

Similarly, total nitrogen content in soil behaves like the total carbon content present. Nitrogen is one of the most mobile nutrients in soil and is abundant in soil, water and air. It is continually cycled among plants, organisms, water, air and soil organic matter through complex biochemical transformations. As most of the nitrogen is held in the organic matter content, its properties and characteristics in soil are common to other organic matter constituents such as

total carbon and phosphorous. These characteristics cause nitrogen to remain at depths closest to roots where it is used by plants. The abundance of nitrogen allows it to be present in all possible sources. Nitrogen inputs are present in precipitation but are generally low and are often assumed to be about equivalent to the annual nitrogen losses through runoff and erosion (NRC 1993).

Chapter 3: Methods

3.1 Introduction

The purpose of this section is to provide a detailed description of the field and laboratory procedures and calculations used throughout this research. Laboratory procedures such as the moisture content, sieve and hydrometer analyses and total carbon and nitrogen analyses will be explained and illustrated through the use of figures and charts. Additional tables and figures are provided in Appendix A-3.

3.2 Soil Sampling

3.2.1 Locating Test Locations

The location of the test locations were identified throughout the basin and other locations such as the berm, to generate a general composition of the soil profile within the basin and surrounding areas. A basic survey of the location of each test location was initially performed prior to sampling the soil profile. Seven test locations were identified. Two test locations were included as standards to represent the existing soil of the site. Using a tape measure and survey pins, the location of these test locations were measured and mapped. The test locations included S1, S2, S3, S4, SED, B1, and B2. An additional test location, O1, was included in this research to analyze a composite eight (8) foot soil profile. The O1 sample was extracted prior to the seven samples and was preserved for future analysis.

S1 represents an area of low elevation in the basin, with frequent traction due to the presence of a single ring infiltrometer and an ultrasonic transducer. S2 is located at the foot of rip rap channel 1 that leads directly to the basin from the parking area. This test location, similar to SI, has a high abundance of vegetation in all four seasons. The S3 and S4 test locations are located in the outlet pipe region of the basin. The test locations are located on either side of the

outlet pipe. The surface area of the S3 test location neighbors a stone bed placed beneath the outlet pipe during construction and harbors incoming flow particulates. S4 is located on the opposite side slope of the S3 area. B1 and B2 test locations are used for standard tests and are located on the either sides of the basin's berm. Unlike other test locations, SED represents a sediment deposit located near the entrance of rip rap channel 1. Similar to S2, this test location represents particulate matter that drains into the site. Figure A shows a detailed mapping of these test locations. Surveying and sampling were carried out during the spring months of 2007 for samples S1, S2, S3, S4 and SED. The surface of the basin was not covered with grass, and vegetation was minimal. This allowed little or no vegetation within the test locations, excluding B1 and B2 due to their location in the grassed berm. These two samples were completed during the summer months. Grass and organic litter such as leaves and twigs were removed in the test location prior to sampling.

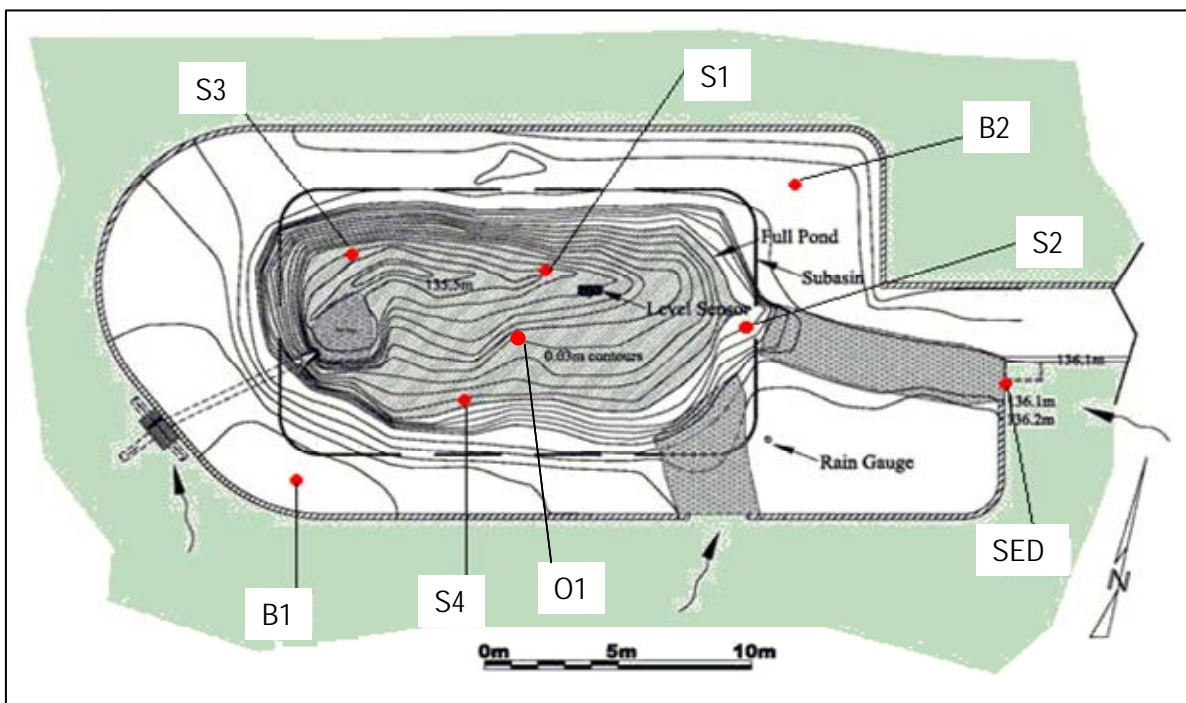


Figure 3.1: Map of Test Locations

3.2.2 Sampling Procedure

The sampling procedure consisted of creating a composite sample for each depth within a test location. The soil was first marked in a 36 in² area for each test location. Extraction points were then marked in the corners and center of the test location. The combination of each extraction refers to a composite sample. Figure 3.2 illustrates the location of each sample comprised in a composite test location.

The Turf-Tec Tabular Soil Sampler (TSS2) was used to perform soil sampling at each test location. The TSS2 is a 36" stainless steel sampler used for analysis of deep soils and determining root depth. It has a $\frac{3}{4}$ " diameter and a 15" opening for viewing a disturbed soil profile sample. A test location represents a composite sample of 5 samples taken from that specific test location. This procedure was developed because the soil sampler is not capable of extracting a large enough quantity from one extraction. Soil samples at these depths are very small in quantity. Each laboratory analysis required a specific mass of soil, therefore the use of a composite sample was implemented into the procedure.

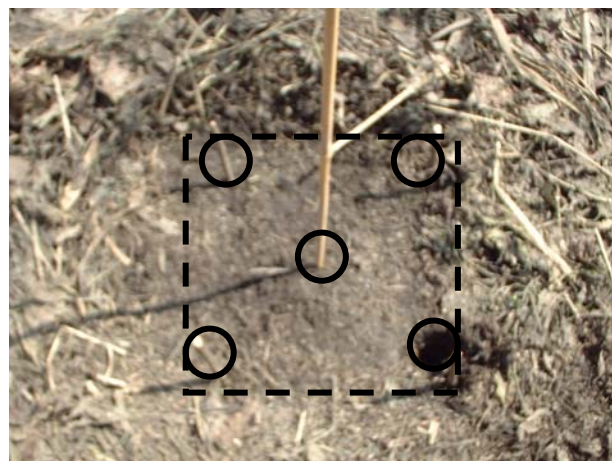


Figure 3.2: Test Location Showing Composite Sample

It was important to remove rocks and other coarse materials in the path of the soil sampler. After insertion into the ground, the sampler must be carefully removed to reduce impact on the soil sample. Once the sampler is removed, only the first foot of the soil sample was analyzed. The sample was then divided into increments for the analysis of soil depth below the surface. A small scoop and length scale were used to measure the corresponding depths and remove the soil from the sampler. Figure 3.3 shows the depths studied and the labeling of each sampled depth.

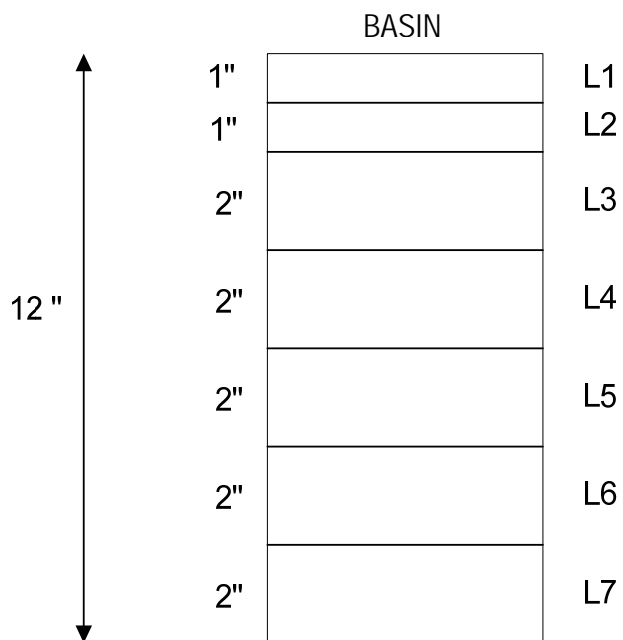


Figure 3.3: Depths for Each Test Location

For each sample, the corresponding layers were bagged individually in moisture proof plastic bags. Sample bags were be returned to a lab within 24 hrs after extraction to preserve the moisture content. Composite samples were created for each layer or depth. Therefore the composite sample for L1 represented five samples of depths of 0-1" bagged together. The total composite samples for test location S1 would comprise of seven samples representing L1, L2, L3, L4, L5, L6 and L7. Figure 3.4 illustrates a sample extraction. For test locations SED, S5 and

S6, sample depths were not measured and analyzed. These samples represented a general soil distribution with no variation in the soil profile or mound of sedimentation. Therefore one composite sample represented the test location for these locations.

In addition to the seven test locations evaluated at the site and additional test location containing four samples was obtained from a previous research experiment. In June 2004, during the installation of three suction lysimeters, four soil samples were retrieved. These samples were obtained at soil at 2, 4, 6 and 8 feet of the basin's profile. This test location was labeled as 01 and can be viewed on Figure 3-1. These samples will represent a full depth through the basin and into the existing subsoil profile at 2 foot increments. Due to the ageing of the soil, tests such as total carbon and nitrogen, and soil moisture content were excluded.



Figure 3.4: Sample Extraction

3.3 Soil Moisture Analysis – ASTM D 2216-90

The composite soil samples were transferred the laboratory for a soil moisture content analysis. This was done within at least 1 hr from the soil extraction for each sample. In the laboratory, large evaporating dishes were initially labeled and weighed. Labeling represented the

test location location and the depth being analyzed. For example a sample at the 11-12 inch depth for test location S2 would be labeled as S2 L7. The soil samples were then placed into the evaporating dishes and weighed. Both initial mass (M_i) and final mass (M_f) of the evaporating dishes were recorded. Once measured, each soil sample is placed in the oven at a drying temperature of $110 \pm 5^\circ\text{C}$ to a constant mass. A constant mass is acquired once the soil sample is dried for a period of 12 to 18 hours. In this case the soil samples were dried over night for 17 hours. The soil is measured immediately after being removed from the oven. Tongs and gloves were used to prevent burning. The soil sample is weighed and recorded as (M_d). Soil water content is calculated using the Equation 1.

$$w = \frac{M_w}{M_s} \times 100 \text{ \%} \quad (\text{Eq.3-1})$$

where :

$$M_w = \text{mass of water present} = M_f - M_d$$

$$M_s = \text{mass of soil solids} = M_d - M_i$$

3.4 Soil Characterization

3.4.1 Particle Size Analysis - Hydrometer Method – ASTM D421, ASTM D422

Each soil sample was characterized through a hydrometer and sieve analysis. Particle size analyses are used to determine the relative proportions of the different grain sizes that make up a statistically representative mass of the soil sample. Statistical representation is used as it is impossible to identify individual particle sizes in a given soil sample. Each analysis is responsible for identifying and distributing varying soil types as they exist in the given sample.

The hydrometer method is used to identify soils ranging from 0.075 mm to 0.001 mm, whereas the sieve method identifies all soil particles greater than 0.075 mm. For the purpose of identifying fine particles comprising of silt and sand grains the hydrometer method was performed initially. This was done to protect fine particles that may have been displaced over the sieving period. The hydrometer method is based on Stokes' Law which gives the relationship among the velocity of falling spheres (soil particles), the diameter of the sphere, the specific weights of the spheres and the fluid and the fluid viscosity. This relationship is explained in Equation 2.

$$v = \frac{2}{9} \frac{G_s - G_f}{\eta} \left(\frac{D}{2} \right)^2 \quad (\text{Eq. 3-2})$$

where :

v = velocity of fall of the spheres (cm/s)

G_s = specific gravity of the sphere

G_f = specific gravity of the fluid – varies with temperature

η = absolute, or dynamic viscosity of the fluid (g/(cm*s))

$g = 980.7 \text{ cm/s}^2$

D = diameter of sphere (cm)

By solving for the diameter, one can accurately assume the presence of specific grains within the soil-water mixture. To solve for D using an assumed specific gravity of water, G_w , at 4°C is 1.0 g/cm^3 the following in Equation 3 is achieved.

$$D = \sqrt{\frac{18\eta v}{G_s - G_w}} \quad (\text{Eq.3-3})$$

Solving Eq. 3 requires the values of velocity, specific gravity of the sphere and fluid as well as the viscosity of the fluid. Through the use of a hydrometer and a thermometer, all factors needed to calculate D can be acquired.

The instruments used for this test include: a 1000 ml hydrometer jar, 1000 ml graduated cylinder for the control jar, 152H model hydrometer, soil-dispersion device, sodium metaphosphate as the dispersion agent, thermometer, evaporating dishes, stop watch and paper towel. The hydrometer used is designated as an ASTM 152H and is calibrated to read from 0 to 60 grams of soil in a 1000 ml soil-water mixture with the limitation that the specific gravity G_s is 2.65 g. The hydrometer displays the specific gravity of the soil-water mixture at the center of the bulb. Soil particles larger than those in suspension in the zone shown as L have fallen below the center of the volume and this constantly decreases the specific gravity of the mixture at the center of volume of the hydrometer. (Fig E). The lower the specific gravity in the mixture becomes, the further the hydrometer moves down. Temperature also influences the specific gravity allowing it to decrease as the temperature rises (Bowles, 1992).

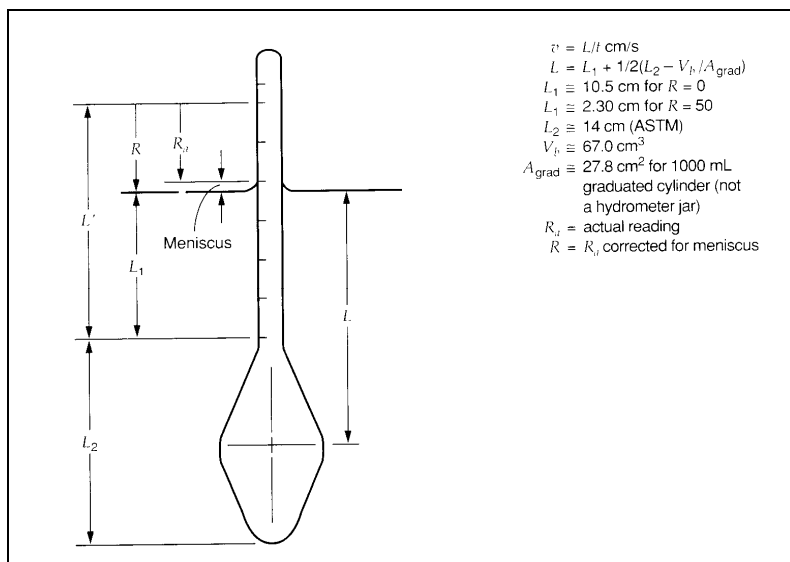


Figure 3.5: Hydrometer Dimensions

The soil-water mixture is made by using 50 grams of the oven dried soil sample. A 4 percent sodium metaphosphate solution is then made by mixing 40 grams of the dry chemical with enough water to make 1000 ml of solution. 125 ml of this solution is then added to the 50 g soil sample and allowed to stand for 1 hr for soaking. The evaporating dish containing this mixture must be covered with wet paper towel to prevent evaporation. During the soaking period, a control jar of the sodium metaphosphate solution is prepared. This is done by preparing a similar solution of 125 ml of a 4% sodium metaphosphate and adding 1000 ml of temperature stabilized water. It is important that the control jar and hydrometer jar maintain temperatures within 1⁰ C. Both the hydrometer and thermometer must be placed in the control jar to maintain a stabilized temperature. After the soaking period is completed, the mixture is added to a dispersion cup and water is added to two-thirds full. The mixture is then dispersed for 1 minute.

After mixing, the mixture is then poured into the hydrometer jar making sure that all the contents are transferred from the dispersion cup. A plastic squeeze bottle is used to rinse all contents of the dispersion cup to the hydrometer jar. Temperature stabilized water is then added to the hydrometer jar to the 1000 ml marking. Using a No. 12 stopper, the jar is sealed and carefully agitated for 1 minute. It is important the contents of the bottom of the jar be suspended into the solution during this time. The hydrometer jar is then set down on a leveled surface and the stopper is removed. Particles should not remain on the stopper or above the 1000 ml volume marking. See Figure 3.6. Temperature is recorded once the jar has been set down.



Figure 3.6: Hydrometer Jars and Control Jar During Testing

The first reading was recorded 1 minute after the jar was set down. At 30 seconds prior to the reading time, the hydrometer was placed in the solution to allow stability. At the reading time the hydrometer reading is recorded and the temperature is measured and recorded. The actual reading of the hydrometer (R_a) is read on the top of the meniscus. Both instruments should be removed from the solution after the reading, and placed in the control jar. This step is repeated for the allotted times of 2,4,8,15,30,60,120,180,300,1200, and 1440 minutes after the initial reading at 1 minute. The hydrometer and thermometer are removed from the solution in between each reading.

In order to satisfy Equation 3, the calculations were carried out to fulfill each factor. A corrected hydrometer ready (R_c) must first be calculated before continuing all computations. See Equation 4 below.

$$R_c = R_a - \text{zero correction} + C_T \quad (\text{Eq.3-4})$$

where

R_c = Corrected hydrometer reading (cm)

R_a = Actual hydrometer reading (cm)

C_t = Temperature correction, Table A in Appendix A-3.

The percent finer at each time step is then calculated using Equation 5. The assumed specific gravity G_s of the soil particles present is 2.70.

$$\% \text{ Finer} = \alpha R_c / M_s \quad (\text{Eq.3-5})$$

where

α = Correction factor for unit weight of solids, Table B

R_c = Corrected hydrometer reading (cm)

M_s = Mass of soil used (g)

The corrected meniscus hydrometer reading (R) is calculated by adding 1 to the value of the actual hydrometer reading. See Equation 6.

$$R = R_a + 1 \quad (\text{Eq.3-6})$$

In order to calculate velocity which is directly related to D , the values for effective depth is calculated for diameters of particles using Stokes' formula. Table C illustrates the corresponding L values with respect to the meniscus corrected readings.

The particle velocity (v) is then calculated as,

$$v = L/T \text{ (cm/min)} \quad (\text{Eq.3-7})$$

With the assumed specific gravity G_s and the recorded temperature of the soil-water solution during the test, the K value is generated through Table D.

Using the K and particle velocity values, the particle diameter is computed using the following,

$$D = K \sqrt{v} = K \sqrt{L/T} \text{ (mm)} \quad (\text{Eq.3-8})$$

Dates, time elapsed, temperature, actual and corrected readings, percent finer, values for L and K as well as the D, are all recorded used to produce a soil grain distribution chart for the fine particles present in the soil sample.

3.4.2 Determining Quantity of Sand

This procedure required the use of the previous experiment's soil-water solution samples, a No.200 sieve pan, a spatula, a 105°C oven, a large bowl, a measuring scale and water supply. The purpose of this experiment was to quantify the mass of sand particles presence at each soil depth. Using the soil-water solution samples from the hydrometer analyses, the hydrometer jar were agitated to allow all particles to be suspended in solution. The No.200 sieve pan and the large bowl were both measured (M_i) and placed together to allow the liquid contents of the hydrometer jar to be contained in the bowl. Soil particles passing the No.200 sieve pan are silt and clay particles. The contents of the jar was poured into the No.200 sieve pan and allowed to strain through to the large bowl beneath. See Figure 3.7. Particles remaining in the hydrometer jar after the pour were removed using water from a plastic squeeze bottle.



Figure 3.7: Collection of Sand Particles on No. 200 Sieve

The contents remaining on the No.200 sieve was thoroughly washed using the plastic squeeze bottle. The sieve pan and the large bowl are separated, and each is measured for wet weight (M_w). See Figure 3.8. It was important that the contents of the sieve be thoroughly washed so that water passing through did not have a brown color.

Once weighed, both the large bowl and the sieve pan are placed in the oven at 105°C . Both containers are allowed to dry over night at this constant temperature. The dried containers are measured and recorded as dried weights (M_D). The mass of sand (M_F) particles retained on the sieve represents the quantity of sand particles present at depth sampled. Equation 9 shows the formula used to calculate the mass of sand (M_F) at each depth. Equation 10 shows the formula used to calculate the mass of fine particles present at each depth.

$$M_s = M_D - M_i \quad (\text{Eq.3-9})$$

where

M_s = mass of sand (g)

M_D = mass of dried pan and sands (g)

M_i = mass of pan (g)

$$M_F = M_D - M_i \quad (\text{Eq.3-10})$$

where

M_F = mass of fines (g)

M_D = mass of dried bowl and fines (g)

M_i = mass of bowl (g)



Figure 3.8: Fines and Sand Contents after Wash & Weighing of Sand Contents

3.4.3 Particle Size Analysis - Soil Sieve Test - ASTM D421, ASTM D422

To achieve a particle size distribution of the sand particles obtained in the last test procedure, soil sieve analysis was performed. A statistical representation of a sieved soil mass is obtained through size bracketing by approximating the size range between two sieves. Size bracketing is done by stacking a stack of sieves ranging in aperture size from the largest at the top to the smallest and sieving a known quantity of material through the stack. This is done by placing the material on the top sieve and shaking to separate the particles into smaller diameters from the top to the bottom. The diameters of the soil particles in the mass of soil retained on any sieve have smaller diameters than the mesh openings of any of the sieves above this one. They are also larger than the smaller mesh openings of any of the sieves below (Bowles, 1992). Each sieve pan represents a mesh opening reflective of a soil grain size. Table D shows the US standards for sieve pan mesh openings.

For the purpose of this experiment the No. 4, 10, 20, 40, 100 and 200 sieves were organized in this order to determine the distribution of soil particles per sample analyzed. A pan

was also placed beneath the No. 200 pan to allow passing particles to be collected. It was important to remove any particles stuck to the mesh openings on the sieve pan. Each sieve pan was measured and the initial weight (M_I) is recorded.

Sieve No.	NOMINAL OPENINGS IN.	STANDARD M.M.
NO.4	0.187	4.75mm
NO.10	0.0787	2.00mm
NO.20	0.0331	840um
NO.40	0.0165	425um
NO.100	0.0059	150um
NO.200	0.0029	75um

Table 3.0: US Standard Sieve Sizing

The sand contents from the previous experiment were then poured into the top sieve (No. 4). A cover was placed on the top sieve and the stack of sieves is placed into a shaker. The shaker was responsible for agitating the stack of sieves, allowing the particle sizes to be distributed. The shaker was set for a time of 5 minutes and sieves were allowed to agitate for that time period. When completed the stack was disassembled into individual sieves. It was important to maintain the contents of the sieves from falling out. Each sieve was then weighed and the final weight (M_F) was recorded. Similar to the hydrometer test, percent passing of each soil particle as well as the corresponding diameter was needed to effectively create a distribution curve for the sieve results. The distribution curve was created by plotting the percent passing against the soil particle diameters for the No. 4, 10, 20, 40, 100 and 200.

The following equations were used to calculate the percent passing of soil particles for their given diameter size. For each sieve pan, the mass retained is calculated using Equation 11.

$$\text{Mass retained (g)} = M_R = M_F - M_I \quad (\text{Eq.3-11})$$

Percent of mass retained is then calculated,

$$\text{Percent of mass retained (\%)} = P_{PR} = \frac{M_R}{M_S} \times 100\% \quad (\text{Eq.3-12})$$

Using the values of percent of mass retained, the percent passing is calculated,

$$\text{Percent passing (\%)} = P_p = 100 - P_{PR} \quad (\text{Eq.3-13})$$

where:

M_F = mass of fines (g)

M_I = mass of bowl (g)

M_s = mass of sand (g)

3.5 Hydraulic Conductivity Analysis

A composite particle distribution curve was created using percent passing (finer) and diameter size values generated from the hydrometer and sieve analyses. A semilog plot was used to generate the curve to include both small and large particle sizes. The percent passing was always plotted as the ordinate using the arithmetic scale. For the purpose of this research, the grain size diameter on the horizontal axis decreases from left to right in log decrements of 10. Results for the hydrometer and sieve analyses were plotted as individual curves and a composite curve was created by combining both curves. To produce a smooth line, a line of best fit was drawn to incorporate as many points on both hydrometer and sieve curves. The initial step for determining the hydraulic conductivity empirically required the values of D_{60} and D_{17} for the combined distribution curve. D_{60} represents the diameter size for a percent passing of 60 percent, and was acquired through linear interpolation when the exact value was not available. Similarly, D_{17} represents the effective diameter and was obtained through interpolation. For cases where

the lowest percent passing value is greater than 17 percent, the lowest diameter value for the corresponding percent passing was used.

The hydraulic conductivity was determined using the Sauerbrei empirical formula as seen in Equation 3-14. The porosity and kinematic coefficient of water viscosity factors are both dependent on the temperature of the soil-water solution. Each sample required varying values of porosity and kinematic coefficient of water viscosity as temperature varied for each hydrometer test performed. For temperature readings that were not directly acquired from the charts, a linear interpolation was performed for values needed.

$$K = \frac{g}{\nu} \cdot C_z \cdot \frac{n^3}{(1-n)^2} \cdot \tau \cdot d_e^2 \quad (\text{Eq.3-14})$$

where,

K = hydraulic conductivity (cm/s)

$g = 9.81 \text{ m/sec}^2$

ν = kinematic coefficient of water viscosity (m^2/sec)

$C_z = 3.75 \times 10^{-3}$

n = porosity = $0.255(1 + 0.83^n)$

η = coefficient of grain uniformity = $\frac{D_{60}}{D_{10}}$

τ = temperature correction. Table F

d_e = effective diameter = D_{17} (or lowest D value)

The resulting hydraulic conductivity values for each sample within a test location were graphed to show comparisons at varying depths within the soil profile. These graphs are illustrated in the Results section.

3.6 Total Carbon and Nitrogen Combustion Analysis

Total carbon and nitrogen within a given sample was analyzed using the LECO TruSPEC CN Determinator. This instrument is capable of determining the carbon and nitrogen content in soil, food, fertilizer and plant samples. There are three phases of this instrument's operation: purge, combust and analyze. In the purge phase, the encapsulated sample is placed in a loading head where it is sealed and purged of any atmospheric gases that have entered during the sample loading. All gas lines and the ballast volume are purged during this time. The sample is then released in a hot furnace at 950 °C during the combustion phase. The sample is flushed with oxygen for very rapid and complete combustion. The by-products of the combustion phase are transferred to a secondary furnace at a temperature of 850 °C for further oxidation and particulate removal. An additional furnace filter and a two-stage thermoelectric cooler remove moisture from the sample. The combustion gases were then collected in a collection vessel known as the ballast (LECO Manual, 2004).

In the ballast, oxygen is injected and mixed with the combustion gases. The homogeneous combustion gases in the ballast are then purged through the CO₂ infrared detector and the 3cc aliquot loop. Once the gases have equilibrated, carbon is measured as carbon dioxide by the CO₂ detector. The gases in the aliquot loop are transferred to the helium carrier flow, swept through hot copper to remove oxygen and change NO_x to N₂ and then flow through Lecosorb and Anhydrene to remove the carbon dioxide and water, respectively. A thermal conductivity cell is used to determine the nitrogen content. Using an external PC and a Windows-based software program, the system operation and data produced are managed and illustrated to the user. Data is displayed as weight percentage or in parts per million as determined by the user (LECO Manual, 2004).

Each soil sample for this analysis was crushed using a mortar and pestle. This was done to allow the machine to analyze a uniform soil sample with no clumps or rocks present. For each sample, only 0.1 grams of soil was used. A thin aluminum foil wrap used to encapsulate the soil, was placed in a holder on a weight scale. Soil was then added to the thin wrap and measured at approximately 0.1 grams. Once measured, the thin wrap was then twisted to enclose the soil sample within. It was important to wear gloves throughout this step to prevent and reduce contact with substances on the outside of the thin wrap. Each sample was analyzed with a duplicate sample to improve accuracy in results. Soil standards of $0.198 \pm 0.019\%$ and $2.99 \pm 0.06\%$ were used to calibrate the samples for nitrogen and carbon, respectively. The standards were prepared similar to the samples, and ran before each new sample test location. Samples were placed in the loading head carousel in groups of 30. The machine was then commanded to begin analysis using the software program. The completion of each combustion allows the program to record both carbon and nitrogen values in percent weight.

Chapter Four – Results

4.1 Introduction

This section presents of the results gathered from the experiments and analyses as described in Chapter 3 for test locations S1, S2, S3, S4, SED and the 8 ft. soil profile samples. The results reflect data for samples collected at least 72 hours prior to any rainfall. Results for the hydrometer, sieve and soil moisture content tests are illustrated in tabular and graphical format. Calculations and other analyses used to determine hydraulic conductivity are also briefly explained in this section. Supporting calculations for hydraulic conductivity are found in

Appendix A-4. Graphical results of the total nitrogen and carbon combustion tests are also be included.

4.2 Soil Moisture Content

The results for soil moisture content for test locations S1, S2, S3 and S4 are represented in Figure 4.0.

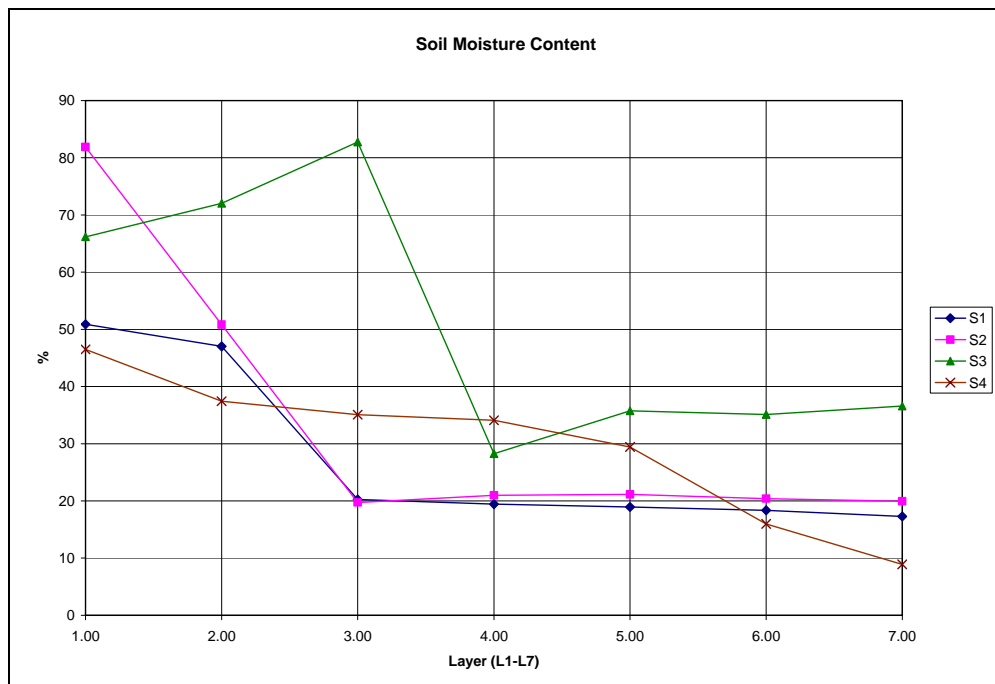


Figure 4.0 – Soil Moisture Content Results

The horizontal axis represent layers L1 through L7, while the vertical axis shows the percent moisture content present in each sample. The plot illustrates test locations S1, S2, S3 and S4. This shows an overall gradual decrease in moisture content as depth lowers into the soil profile. There was an increase in moisture from 0 in. to 4 in. of depth below the surface for test location S3. From 4 in. to 6 in. below the surface, moisture reading decrease to levels comparable to the other three test locations. Another slight increase is then visible from 6 in. to 8 in. below surface, where the moisture continues downward at a constant level. Samples at S3 maintained higher

moisture content compared to S1, S2, and S4. High moisture levels for S3 can be associated with its location nearest to the outlet, which is typically wet compared to other locations in the basin. Although the soil content at each test location varied, a similar pattern in moisture distribution was apparent.

4.3 Particle Size Analysis

As described in Chapter 3- Methods, particle size analyses, hydrometer and sieve tests, were conducted at seven sample layers for each test spot. Table 4.0 shows each sample evaluated for the corresponding test location. Note that layer L1 was not evaluated for particle size analysis in all four samples within the basin because of high levels of organic litter. L2 and L3 in sample S3 were also excluded because of to high organic content at both depths. However, all layers were analyzed for soil moisture, and total carbon and nitrogen content for S3.

Test Spot	Sample Layer	Width (in)	Test Spot	Sample Layer	Width (in)	Test Spot	Sample Layer	Width (in)	Test Spot	Sample Layer	Width (in)
S1	L2	1	S2	L2	1	S3	L3	2	S4	L2	1
	L3	2		L3	2		L4	2		L3	2
	L4	2		L4	2		L5	2		L4	2
	L5	2		L5	2		L6	2		L5	2
	L6	2		L6	2		L7	2		L6	2
	L7	2		L7	2					L7	2

Test Spot	Sample Layer	Width (in)
SED	---	---

Test Spot	Sample Layer	Width (in)
B1	---	---

Test Spot	Sample Layer	Width (in)
B2	---	---

Test Spot	Sample Layer	Width (in)
O1	F2	24
	F4	48
	F6	72
	F8	96

Table 4.0 – Test Spots and Samples

4.3.1 Hydrometer Method Calculations

To create the hydrometer portion of the particle size distribution curve, the results from the hydrometer analysis were calculated using Eqs 3-4 to 3-8 from Chapter 3. Table 4.1

illustrates the results for L7 in test spot S1. The results for each sample are shown in Table 4.1.

Additional data is available in Appendix A-4.

SAMPLE	S1										
LAYER	L7										
CALGON SOLUTION AMT.	125ML										
MASS SOIL (g)	50.2										
DATE & TIME OF READING											
DATE & TIME OF READING	TIME	ELASPED TIME	TEMP C	ACTUAL HYD. READ	CORR. HYD. READ	% FINE	HYD. CORR.	L	L/t	K	D
		(mins)	(mins)	Ra	Rc		R	(cm)	(cm/min)	mm(min/cm)^1	(mm)
4/19/07 13:14	0:00		17								
4/19/07 13:15	0:01	1	17	33	31.3	61.73	34	10.70	10.700	0.014	0.045795
4/19/07 13:16	0:02	2	17	33	30.97	61.08	34	10.70	5.350	0.014	0.032382
4/19/07 13:18	0:04	4	17	32	29.98	59.12	33	10.90	2.725	0.014	0.023111
4/19/07 13:22	0:08	8	17	30	28	55.22	31	11.20	1.400	0.014	0.016565
4/19/07 13:29	0:15	15	17	28	26.02	51.31	29	11.50	0.767	0.014	0.012258
4/19/07 13:44	0:30	30	17	27	25.03	49.36	28	11.70	0.390	0.014	0.008743
4/19/07 14:14	1:00	60	17	26	24.04	47.41	27	11.90	0.198	0.014	0.006235
4/19/07 15:14	2:00	120	17	25	23.05	45.46	26	12.00	0.100	0.014	0.004427
4/19/07 16:14	3:00	180	17	25	23.05	45.46	26	12.00	0.067	0.014	0.003615
4/19/07 18:14	5:00	300	17	24	22.06	43.50	25	12.20	0.041	0.014	0.002823
4/20/07 10:14	21:00	1260	16.75	24	22.06	43.50	25	12.20	0.010	0.014	0.001378
4/20/07 13:14	0:00	1440	16.75	24	22.06	43.50	25	12.20	0.008	0.014	0.001289

Table 4.1- Hydrometer Calculations

Most tests were carried out over a period of 24 hours, but some tests were extended for as long as 72 hours. Temperature readings were vital to this test and were recorded at each reading. Therefore this example illustrates that over 60 percent finer for the soil sample comprising of fine grained particles. After a 24 hour period the percent finer was only reduced to 44 percent. This supports the fact that the soil sample had high contents of fines still in suspension after the allotted test period. Each calculated percent finer reading reflects a corresponding particle diameter size (Fig 4.1). The hydrometer results are plotted along with the sieve curve and a combined curve.

4.3.2 Sieve Method Calculations

Using Equations 11 through 13 from Chapter 3, the percent finer content was calculated for each sample, similar to the hydrometer results above. The series of sieves correspond to an assigned particle size diameter for each percent finer value. Unlike the hydrometer test, the particle size diameters for a sieve test are standard. Hydrometer test diameters are calculated using the data retrieved from the tests. Percent retained reflects the percent mass of soil saved on each sieve after the agitation process. Results in the upper portion of Table 4.2 shows the majority of the sand particles retained on the No.40 and No.100 sieves. The corresponding particle diameters for these sieves range from 0.42 to 0.075 mm, and are defined as fine-grained sands. The lower portion of this table illustrates the percent passing, or the amount of soil that is not, retained on each sieve. This data and the corresponding diameter size were used to plot this relationship. At each layer for this test location, at least 30 percent of the soil passed the No. 200 sieve or maintains a 30 percent fine particle soil (silt and clay) content.

Sieve	Dia			Percent Retained (g)				
	(mm)	L1	L2	L3	L4	L5	L6	L7
4	4.750		0.00	0.00	1.65	0.00	0.00	0.00
10	2.000		2.75	4.85	9.00	6.02	1.29	0.53
20	0.840		8.88	11.74	14.47	13.66	5.93	14.40
40	0.425		33.60	20.02	19.28	18.76	23.47	21.60
100	0.150		13.70	20.96	18.65	20.96	23.21	21.01
200	0.075		4.76	5.34	3.95	5.44	5.24	5.54

Sieve	Dia			Percent Passing (%)				
	(mm)	L1	L2	L3	L4	L5	L6	L7
4	4.750		100.00	100.00	98.35	100.00	100.00	100.00
10	2.000		97.25	95.15	89.35	93.98	98.71	99.47
20	0.840		88.38	83.41	74.88	80.33	92.78	85.07
40	0.425		54.77	63.38	55.61	61.56	69.32	63.47
100	0.150		41.08	42.42	36.95	40.60	46.11	42.46
200	0.075		36.31	37.08	33.00	35.16	40.87	36.92

Table 4.2 – Sieve Test Calculations for S1 L7

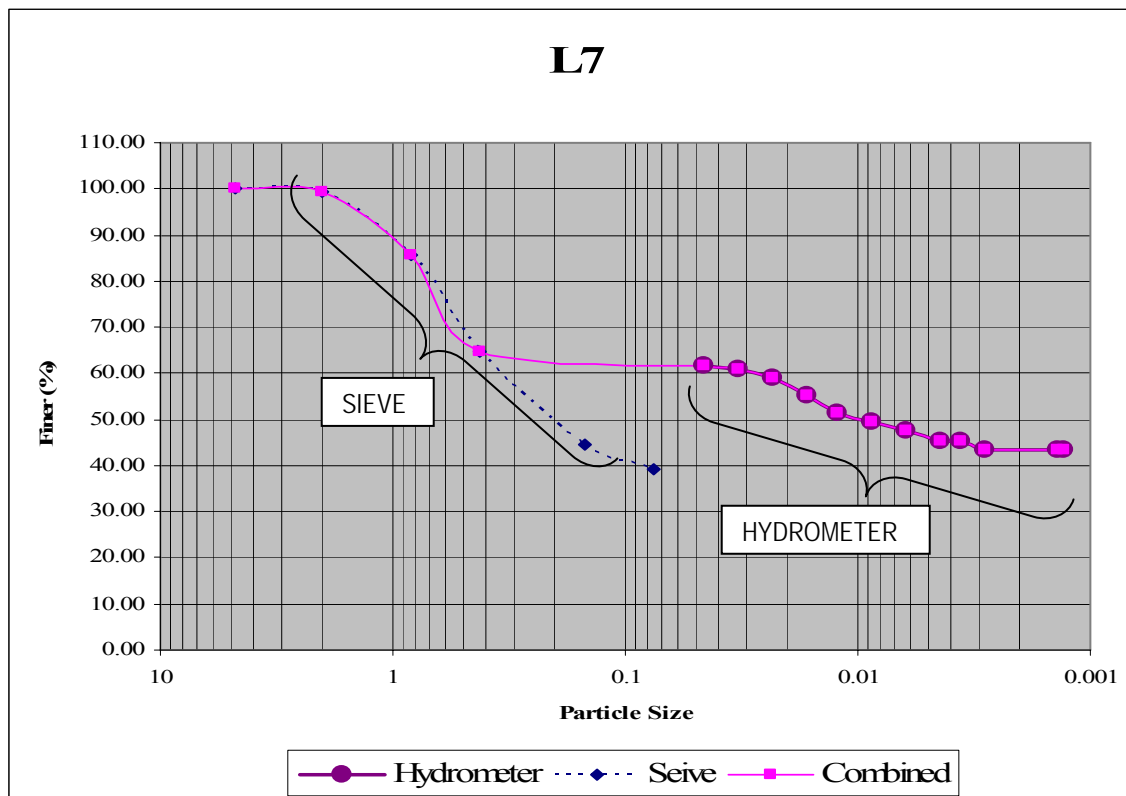


Figure 4.1 – Hydrometer and Sieve Particle Size Distribution Curve for L7

4.4 Fine Particle Content

4.4.1 One Foot Soil Profiles (Test Location S1, S2, S3 & S4) and Sample SED

The total fine particle content at each layer for test locations (L2 to L7) within the basins are represented by the percentage soil passing the No. 200 sieve (Figure 4.1a). The results show a relatively stable distribution of fine particles within the 1 foot profile for locations S1, S2 and S4; with a slight increase in the lowest depths. The average fine particle content along the one foot profile at S1, S2 and S4 is 37, 31 and 38 percent, respectively. However, test location S3 which is located closest to the outlet shows variation from the other three locations, with a decrease from L3 to L6 then a sharp increase from L6 to L7. S3's average fine particle content along the profile is 43 percent. Sample SED which represents the sediment load at the mouth of the riprap channel maintained a fine particle content of 48 percent. Compared to samples evaluated in the basin, SED has the highest fine particle content.

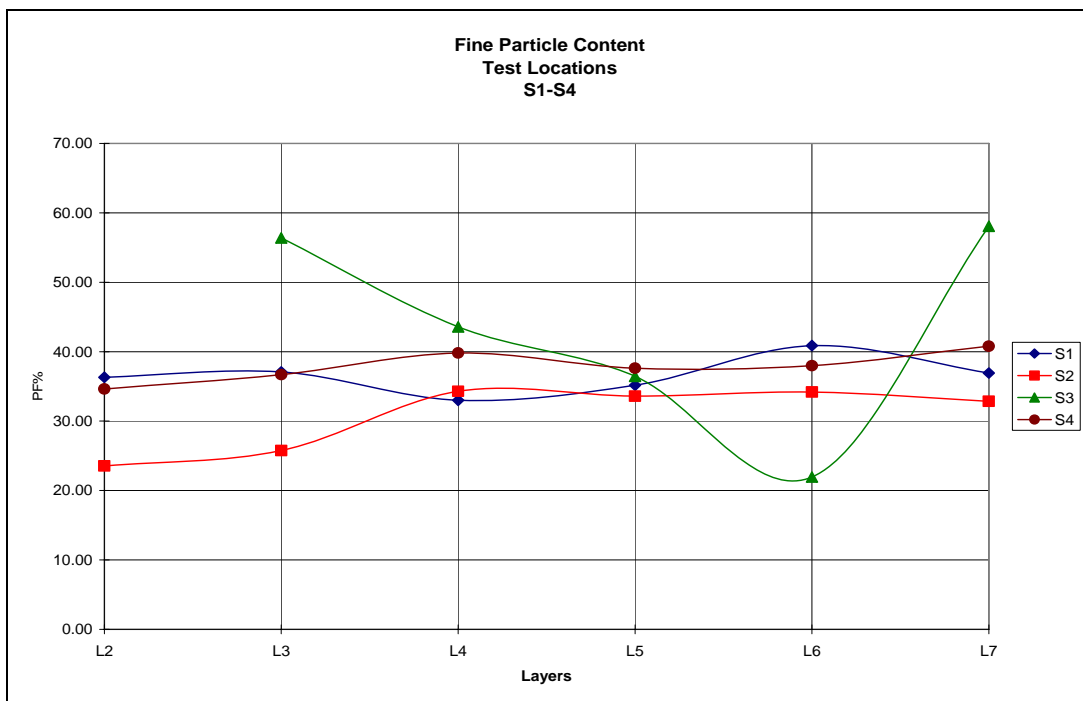


Figure 4.1a – Fine Particle Content for Soil Profile Test Locations S1-S4

4.4.2 Eight Foot Soil Profile (Test Location O1)

Figure 4.1b represents a plot of the fine particle content along the eight foot profile in the basin. The fine particle distribution is relatively constant throughout this profile with a maximum content at the 4 ft. and 6 ft depths. The 2 ft and 8 ft depths along the basin have the lowest fine particle content at 34 and 35 percent, respectively. The average fine particle content distribution along the 8 ft. profile is 36 percent. Similarly, the average fine particle content within the designed profile (2 ft to 4 ft) is 37 percent.

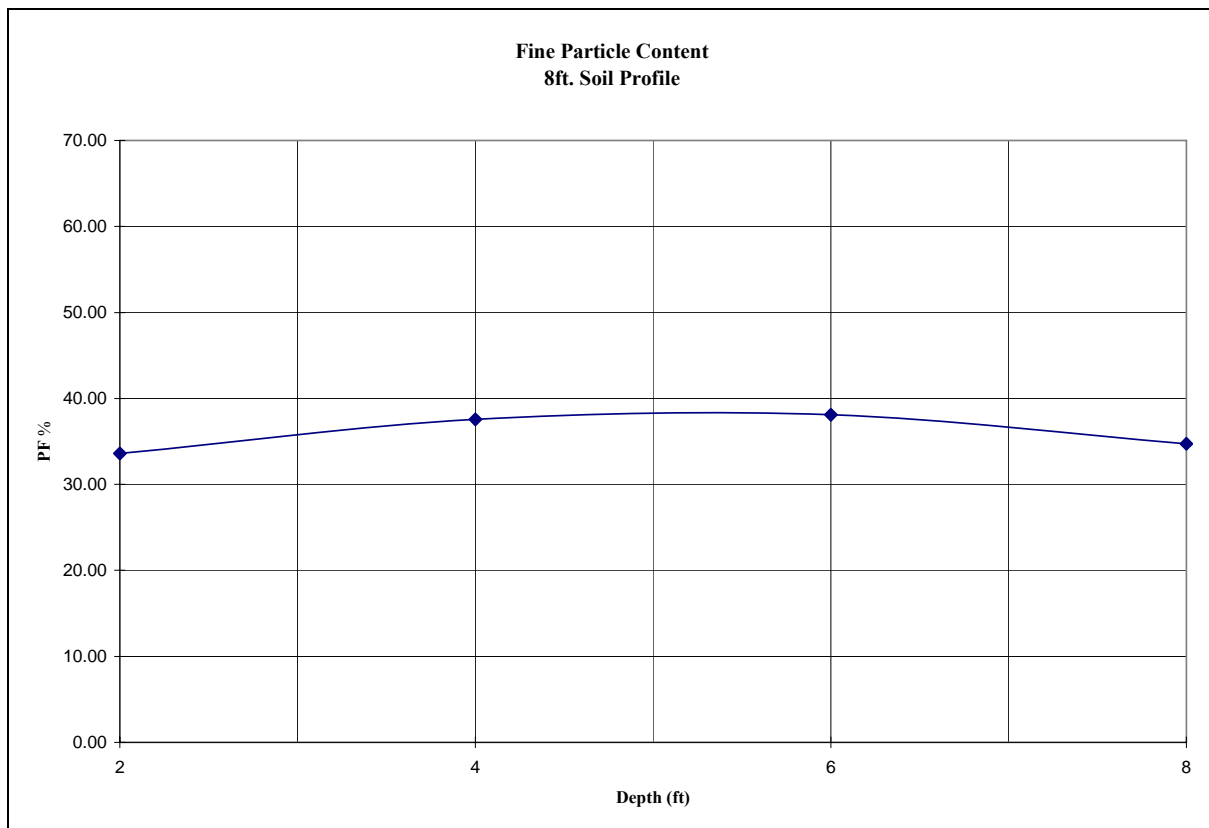


Figure 4.1b - Fine Particle Content for Soil Profile O1

4.5 Grain Size Distribution Curves

The following results represent the soil distribution for silt, clay and sand particles for all samples evaluated.

4.5.1 Test Locations - S1, S2, S3, S4

Figures 4.3, 4.4, 4.5, and 4.6 demonstrate the complete particle size distribution curves for test locations S1, S2, S3 and S4.

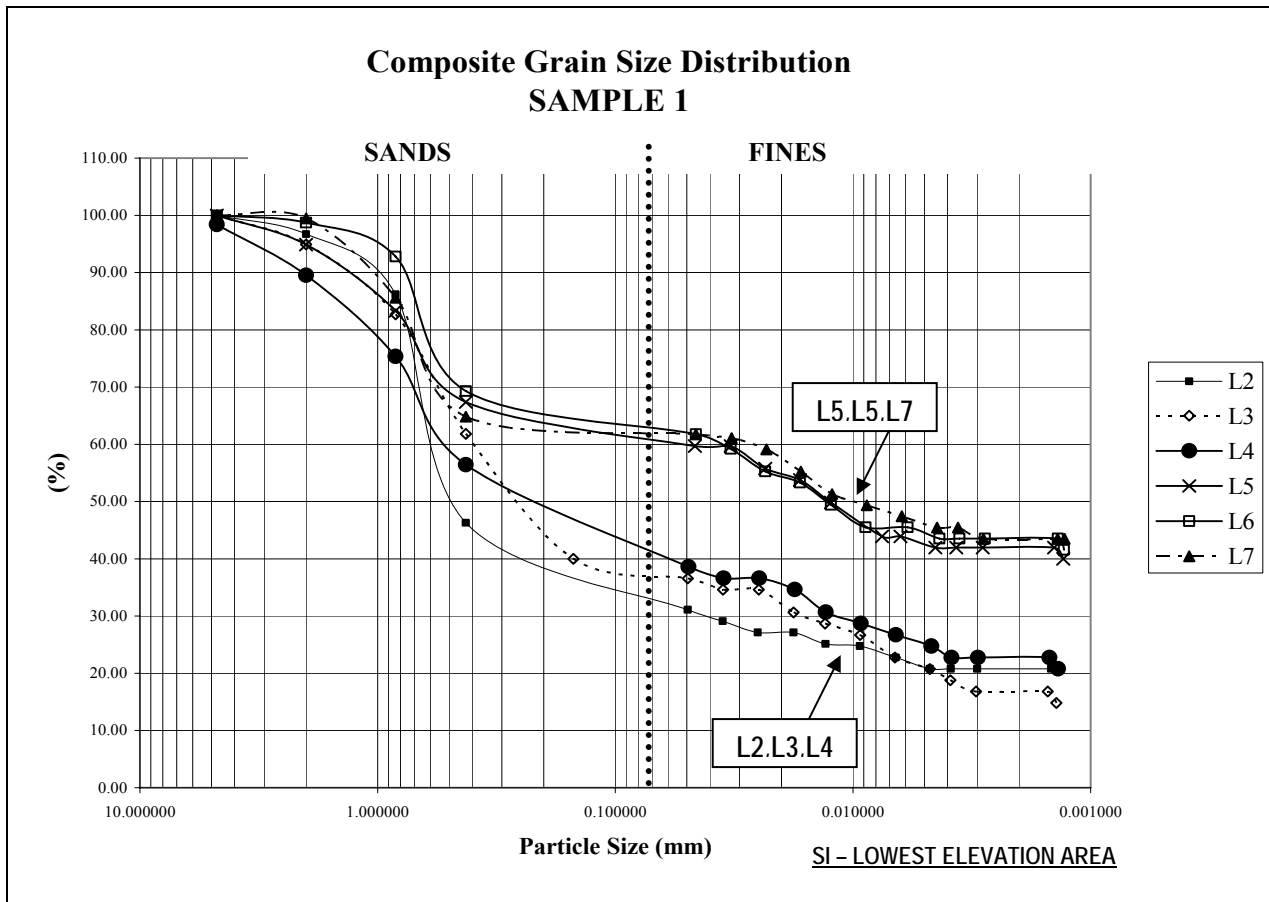


Figure 4.3 – Test Location S1: Grain Size Distribution Curve

The composite curve produced for test location S1 shows a separation at the lower limits or within the fine particle area of the curve. Unlike the other three graphs, this is the only case where this has happened. It shows two groups of layered depths at similar percent passing values

for fine particles. Layers L2, L3 and L4 which corresponds to 2 to 6 inches below the surface; shows lower percent passing values compared to the group above for fine grained particles retrieved from the hydrometer test. The group above consists of layers L5, L6 and L7 corresponding to depths of 6 to 12 inches below the surface. The fine particle distribution for L5, L6 and L7 ranges from 60 to 40 percent. The clay-sized particles also varied in the two portions with ranges of 17 to 23 and 42 to 44 percent in the lower and upper respectively.

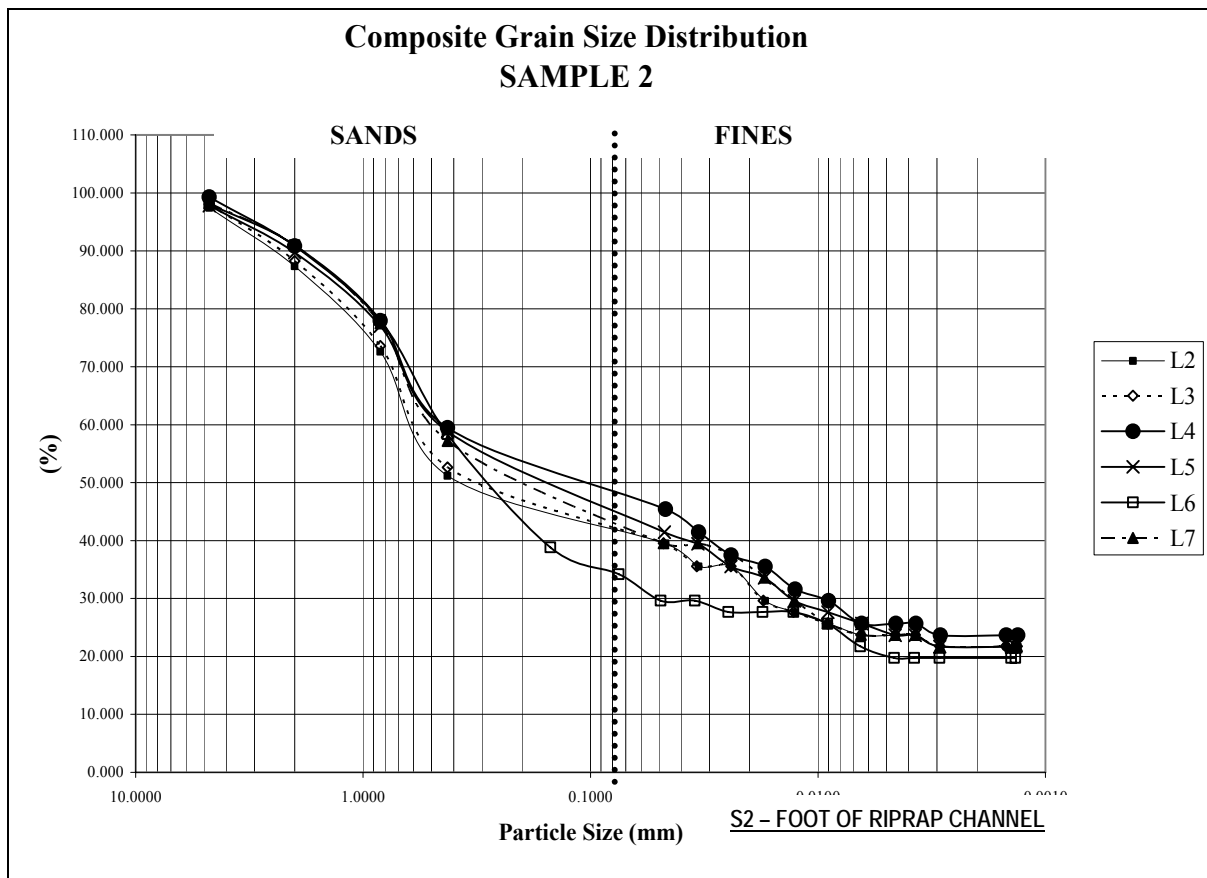


Figure 4.4 – Test Location S2: Grain Size Distribution Curve

Layers at test location S2, which is located at the foot of the rip rap channel, had fairly consistent percentages of fines. Values were between the 40 to 45 percent fines for layers L2, L3,

L4, L5 and L7. The sand portion of the sample also showed comparable results for L2, L3, L4, L5 and L7. L6 demonstrated a small distribution of fine grained sands compared to the other layers. The clay soil content ranged from 10 to 23 percent over the foot profile. Compared to test location S1, this composite sample has a fine particle distribution as much as half of those in L5, L6 and L7 in S1. However, the fine particle distribution from L2, L3 and L4 in S1 are more comparable to the overall distribution at S2.

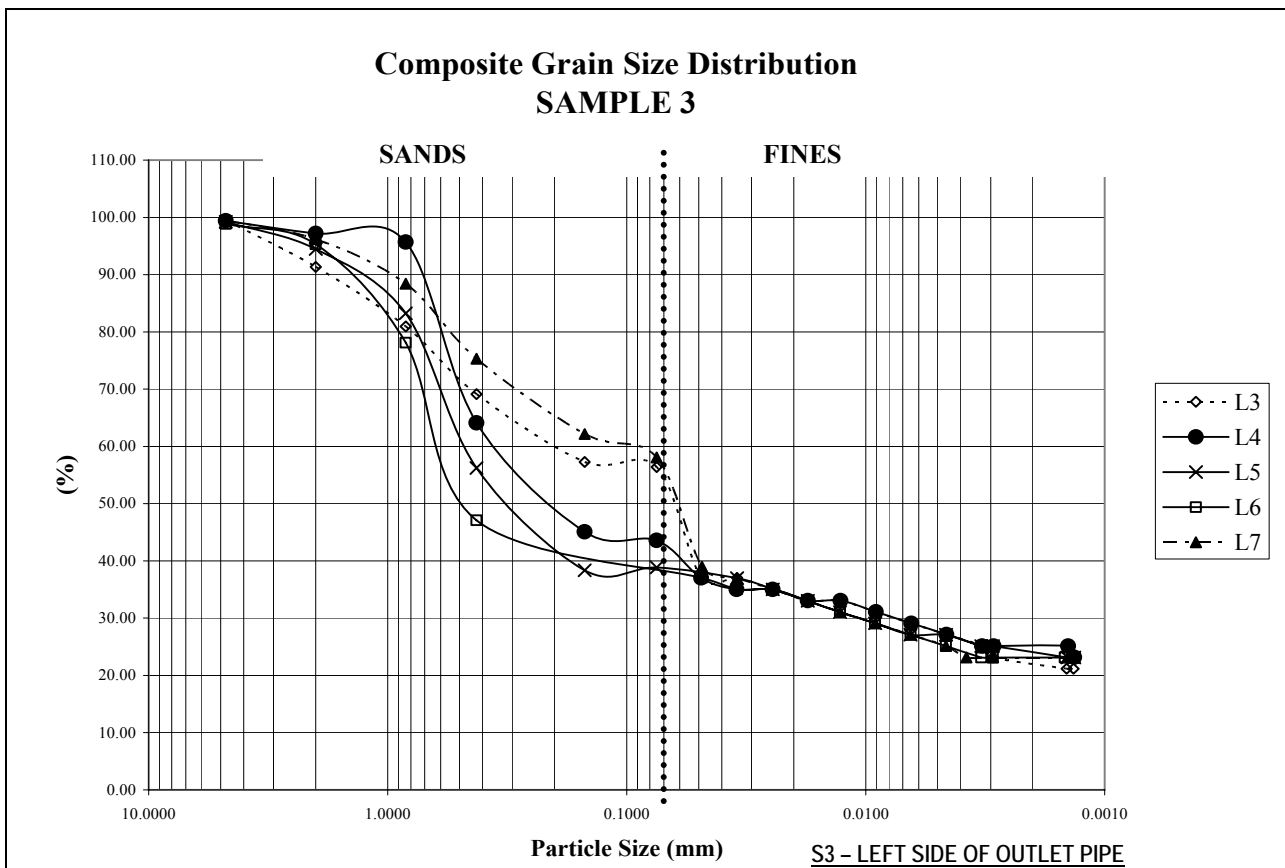


Figure 4.5 – Test Location S3: Grain Size Distribution Curve

For test location S3, the variation was within the sand portion of the each sample. Figure 4.5 illustrates that although the percentage of fines was similar over the one foot profile, the sand portion of each sample differed significantly. Layers L3 to L5 had the least amount of sand

while, L6 and L7 had the highest sand contents. The fine particle distribution for this test location was consistent. The clay-sized particle content was distributed from 23 to 25 percent of the one foot profile studied. Both sand and fine grains of silt and clay for layers L2, L3, L4, L5, L6 and L7 of sample S4 were consistent in distribution (Fig 4.6). The percentage of fine particle soils ranged from 35 to 40 percent. The clay content distribution along this profile was consistent along a range of 23 to 30 percent. The overall grain distribution of each test location is illustrated in Figure 4.7.

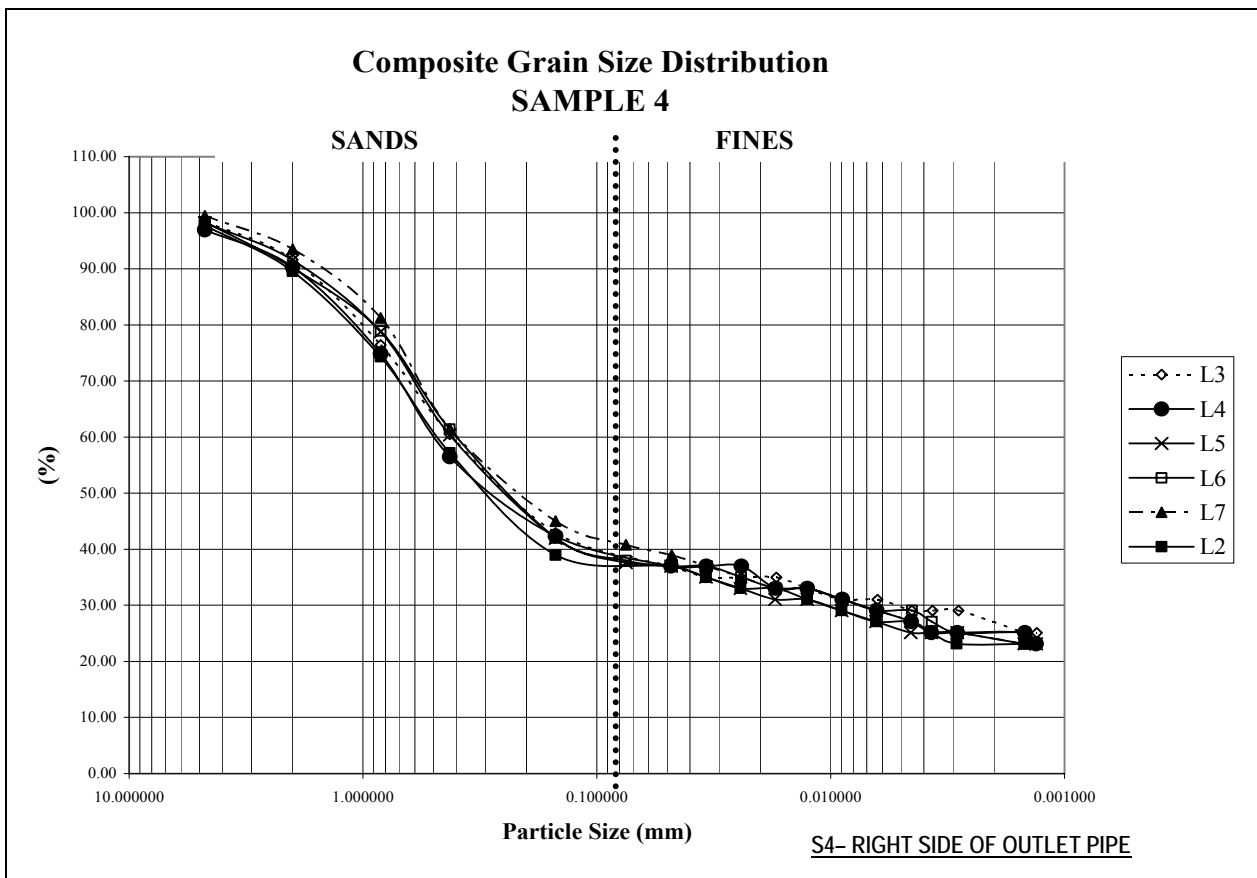


Figure 4.6 – Test Location S4: Grain Size Distribution Curve

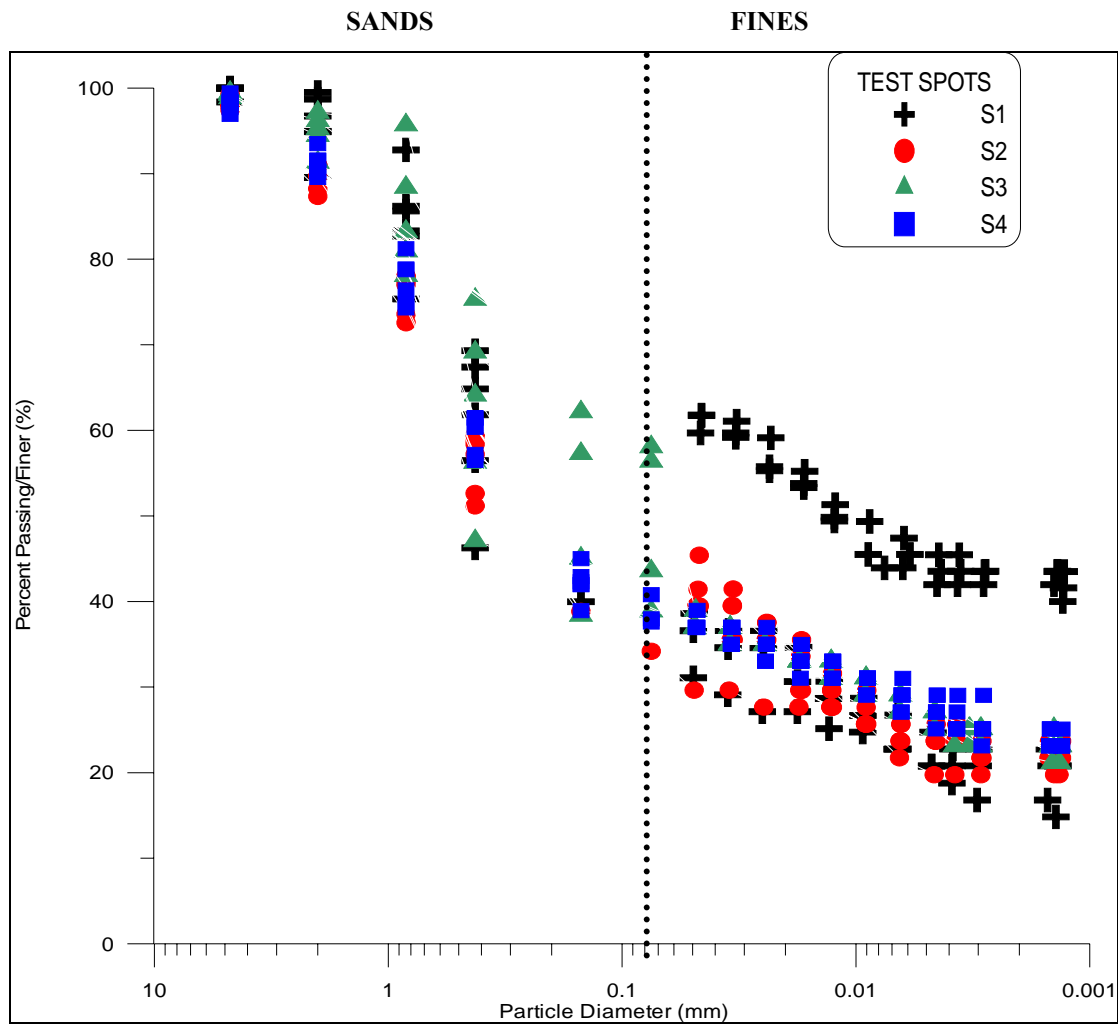


Figure 4.7 – Comparison of Test Location Curves

4.5.2 Sediment Load – SED

Figure 4.8 represents the grain curve for the sediment load sampled at the mouth of the rip rap channel. The percentage of fines for this sample is approximately 48 percent, with 20 percent consisting of clay-sizes particles.

4.5.3 Surrounding Berm Samples – B1, B2

Samples B1 (Fig 4.9) and B2 (Fig 4.10) represent soil samples on the surrounding berm of the basin. Each is located on either side of the other (Fig 3.1). Because a complete particle

size distribution of the original soil was not evaluated during construction, these soil samples are characterized as the existing soil. The percentage of fines for both samples are similar with sample B1 at 55 percent and B2 at 60 percent. The sand distribution is also fairly consistent sizes. The clay fraction is 30 and 33 percent for B1 and B2 respectively. The similarity of the grain sizes of these two samples confirms that the berm's soil is the same all around and that this soil can represent the original soil type of the site as there was no fill added to the surrounding areas during construction.

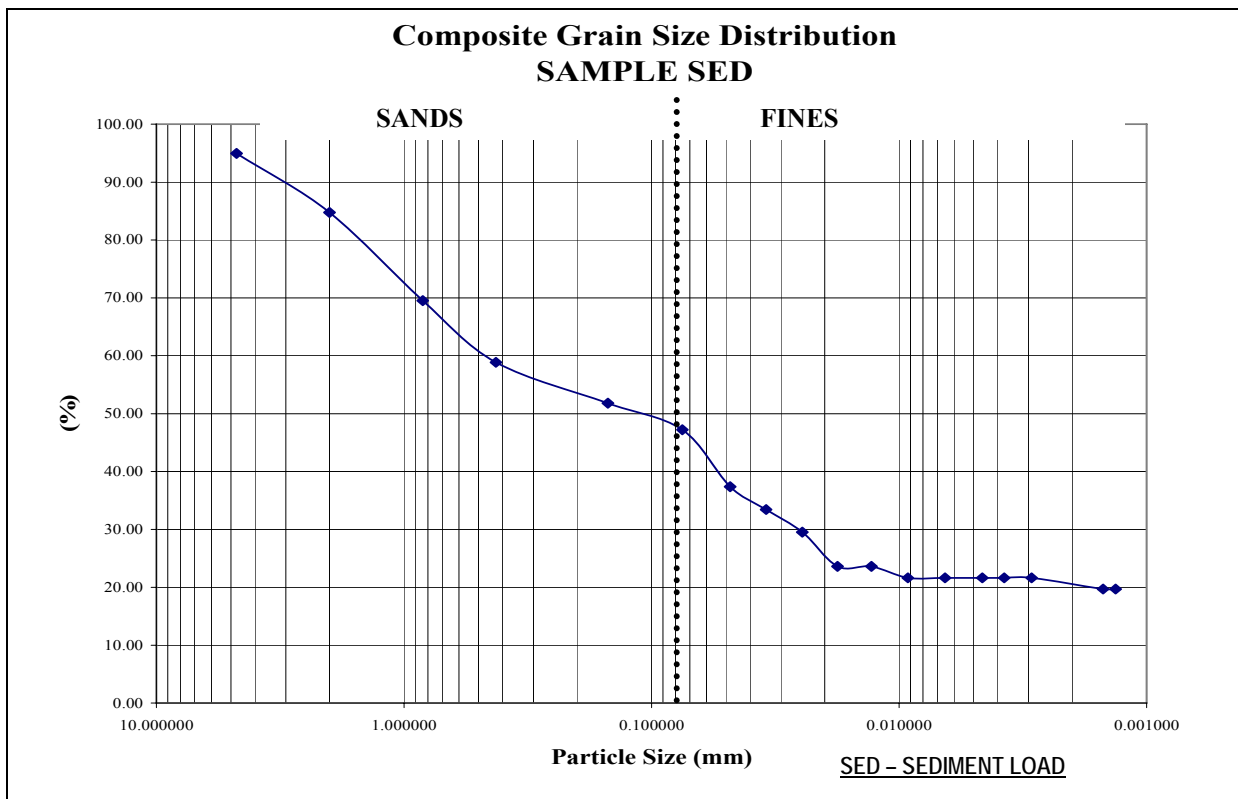


Figure 4.8 – Test Location SED: Grain Size Distribution Curve

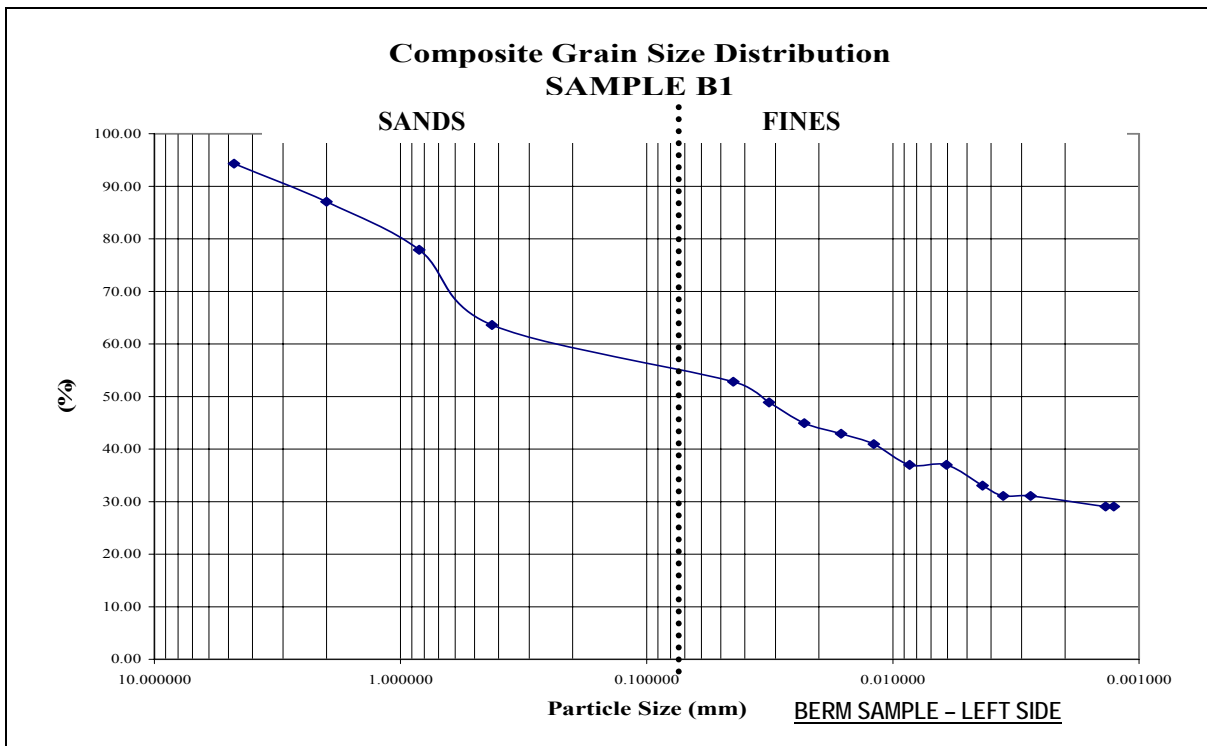


Figure 4.9 – Test Location B1: Grain Size Distribution Curve

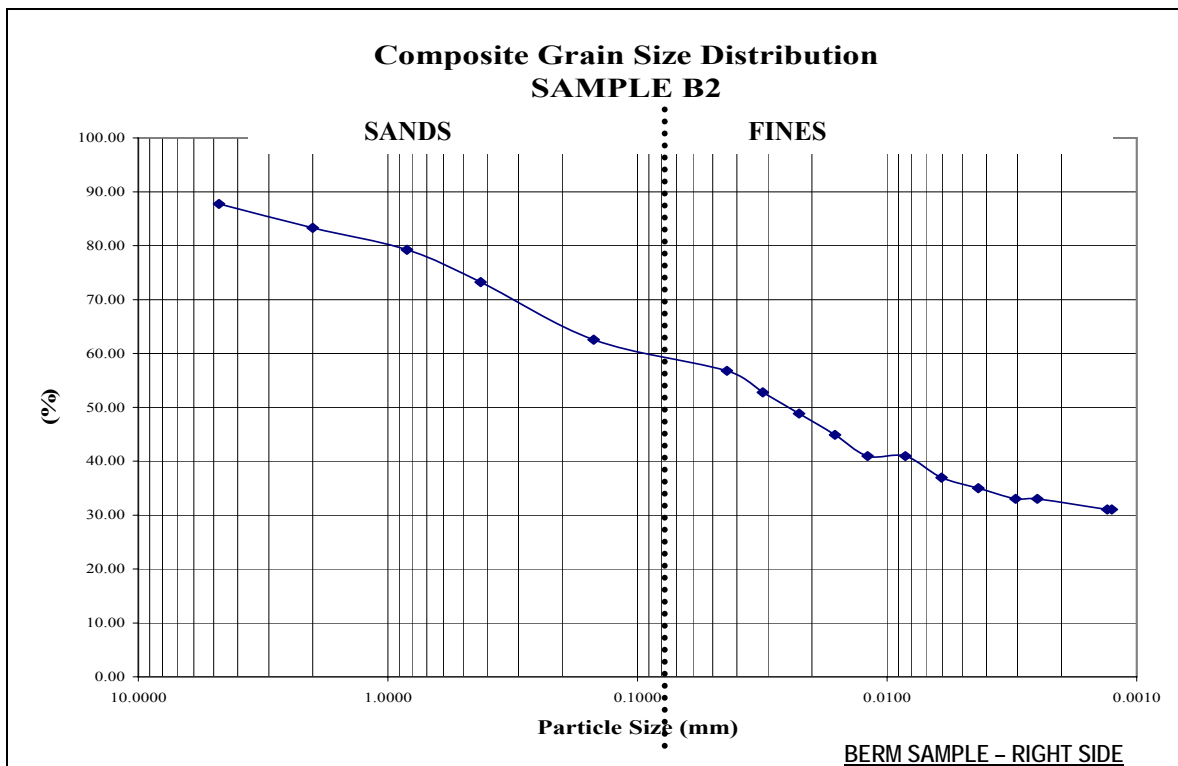


Figure 4.10 – Test Location B2: Grain Size Distribution Curve

4.5.4 Eight Foot Soil Profile Sample – O1

Figure 4.11 shows the plot for soil samples taken at 2, 4, 6 and 8 feet below the surface. Each depth is plotted in the graph below and layers are represented by 2 FT, 4 FT, 6 FT and 8 FT, respectively.

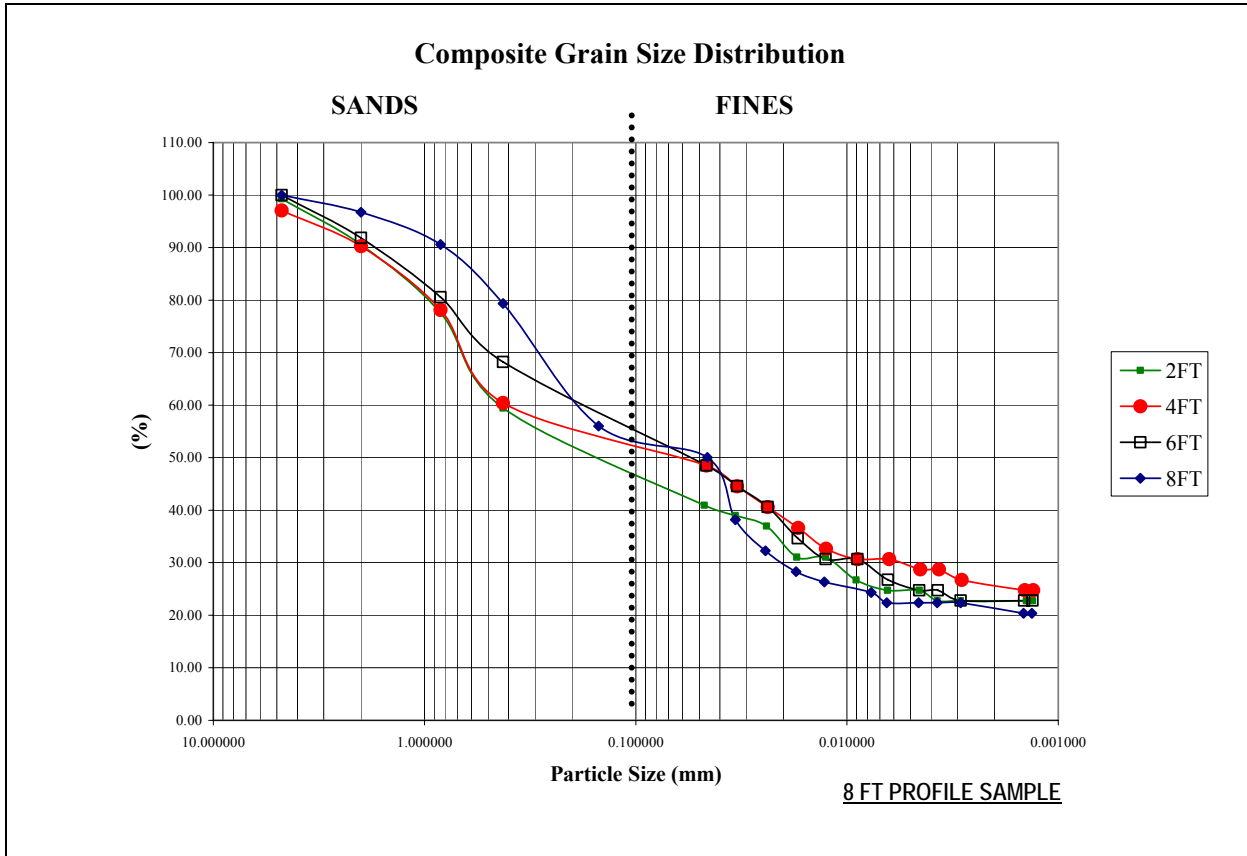


Figure 4.11 – Test Location 01: Grain Size Distribution Curve

The particles size distribution for the eight foot soil profile sample showed similar results to the distribution of the one foot profiles of S1 through S4. Each layer represents 2 foot increments from the surface of the basin. The sand distribution was fairly consistent among the layers except for 8 FT where the sand content was finer than those in 2 FT to 6 FT. 8 FT also stood out as it had the lowest fine particle content of the four layers. This occurrence contradicts that of the previously studied one foot soil profiles where fine particles tended to be more

prominent at lower depths. In this case, the samples 6 FT and 4 FT had the highest fines out of the four layers. The 4 FT sample is from the bottom of the designed soil profile, while 6 FT and 8 FT are from the original soil. The percentage of clay soil content was within 20 to 30 percent for all four layers, with 4 FT having the largest percentage of clay content at 27 percent.

4.5.5 Original (Construction) Sieve Results

A sieve analysis was conducted on the original soil from the site during the construction phase. This was the only particle size distribution test carried out on the existing soil at that time. Figure 4.12 shows the results for the sieve test. The percent finer for particles passing the No.200 sieve was above 55 percent. Although a complete particle distribution would have demonstrated the percentages of both sand and fine particles, test location sample B1 and B2 provide this missing data. Both samples, as mentioned previously, are from a non-filled area around the basin. Using the data from these samples, a valid assumption can be made of the original soil in this area during the site's early stages. Figure 4.13 shows three plots consisting of the original sieve, B1 and B2. The plots show that the original sieve replicates that of sample B2. Therefore, for the purposes of future analyses, B2 will be assumed as the particle distribution of the original soil.

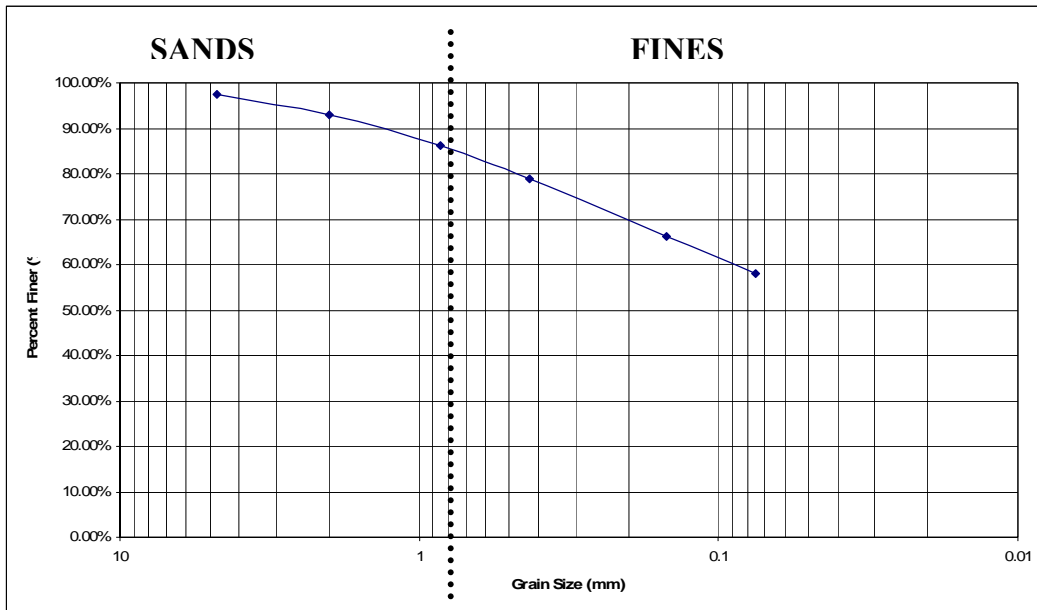


Figure 4.12 – Sieve Analysis Results of Original Soil during Construction

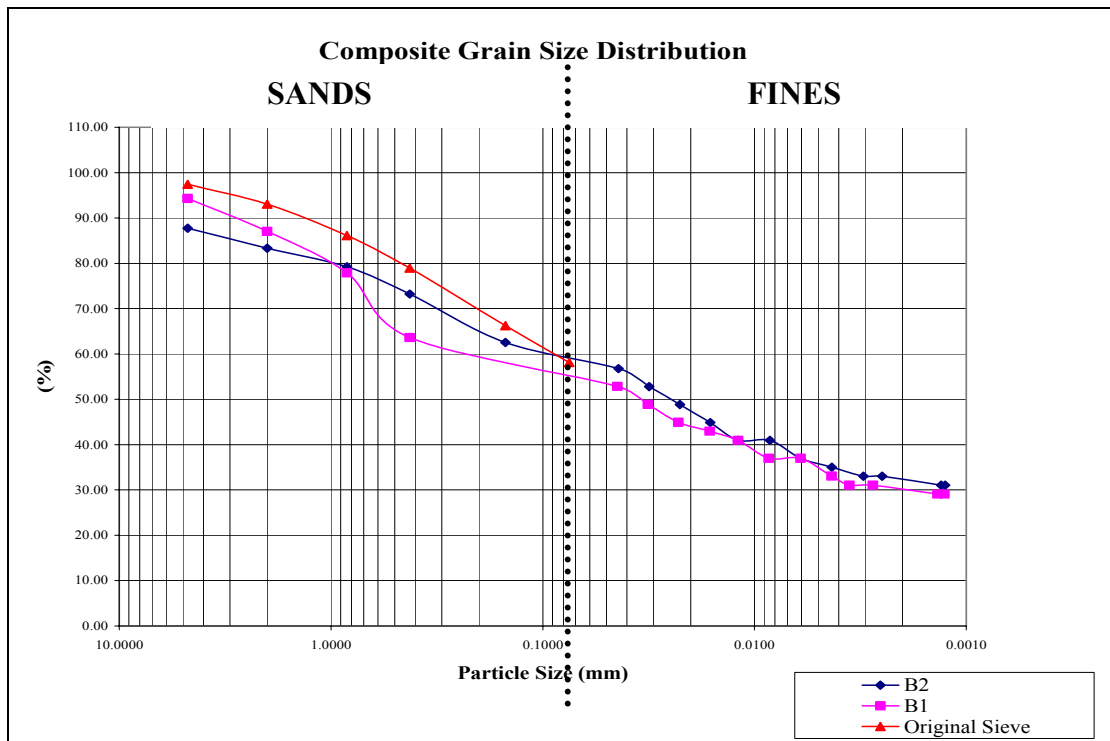


Figure 4.13 – Plots of B samples and Original Sieve

4.6 Calculated Hydraulic Conductivity

Using the equations of the Sauerbrei formula, the particle distribution curve presented in the last section was used to calculate the hydraulic conductivity. An example calculation for S1 L7 is shown in Table 4.3. A graphical representation of hydraulic conductivity for each layer for test locations within the basin is illustrated in Figure 4.14.

L7			
g =	9.81	m/s ²	
v =	1.09E-06	at 17 degrees C	
Cz =	0.004		
τ	0.975	at 17 degrees C	
η =	$d_{60}/d_{10^*} =$	47.50	
n =	$0.255(1+0.83^{\eta}) =$	0.26	
$d_{e17} =$	0.0013		
d_{60}	d_{10^*}		
0.0612	0.0013		
K (cm/s) =	0.0016	K (in/hr) =	2.32

Table 4.3 – Hydraulic Conductivity Calculations

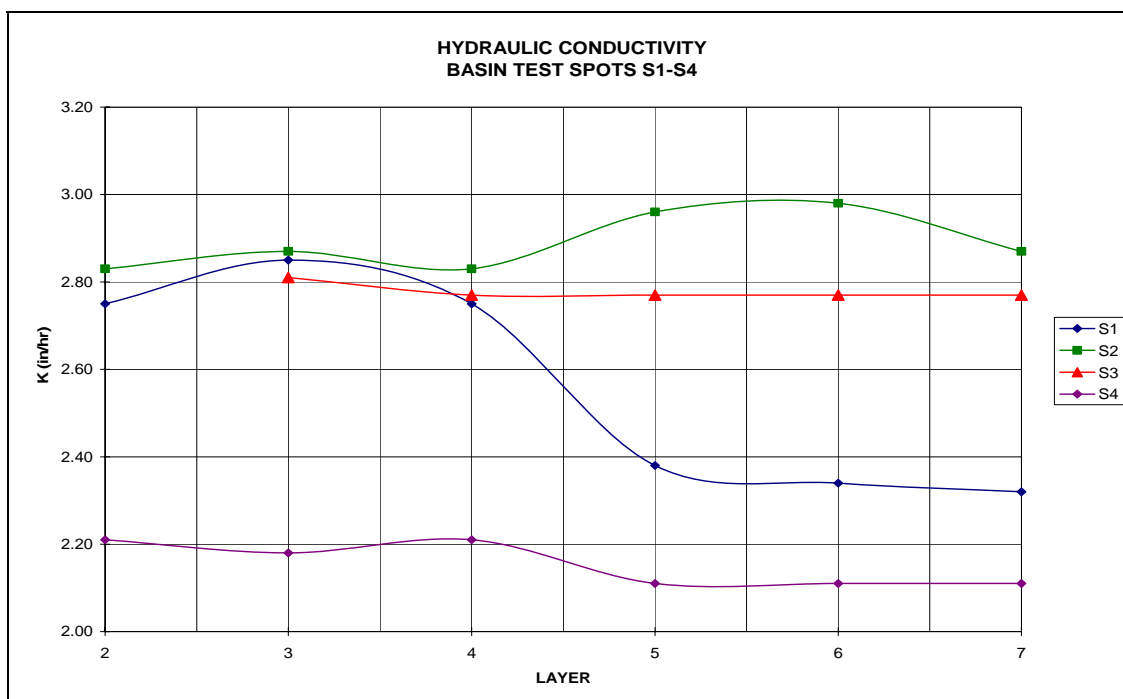


Figure 4.14 – Hydraulic Conductivity Plots for S1-S4

Hydraulic conductivity for each sample excluding S2, decreases with increasing depths in the soil profile. Samples L5 and L6 increased in hydraulic conductivity at test location S2, then decreased to a more constant value. S1 had the largest change in hydraulic conductivity; values dropped from 2.75 in/hr to 2.32 in/hr in 1 foot of soil. S3 had the smallest change, with fairly constant values from L3 through L7.

Figure 4.15 shows a plot of the hydraulic conductivity for test location O1 at layers 2, 4, 6 and 8 feet. This plot shows a decrease in hydraulic conductivity from 2 to 4 feet of depth from the surface. At 4 feet, the soil profile maintains the lowest hydraulic conductivity compared to the other three depths evaluated. From 4 feet onwards, the hydraulic conductivity steadily increases to a rate of 2.87 in/hr. This pattern reflects the particle size distribution for O1. In Figure 4.11, L8 had the lowest percentage of fine particles causing it to uphold the lowest range for percent passing.

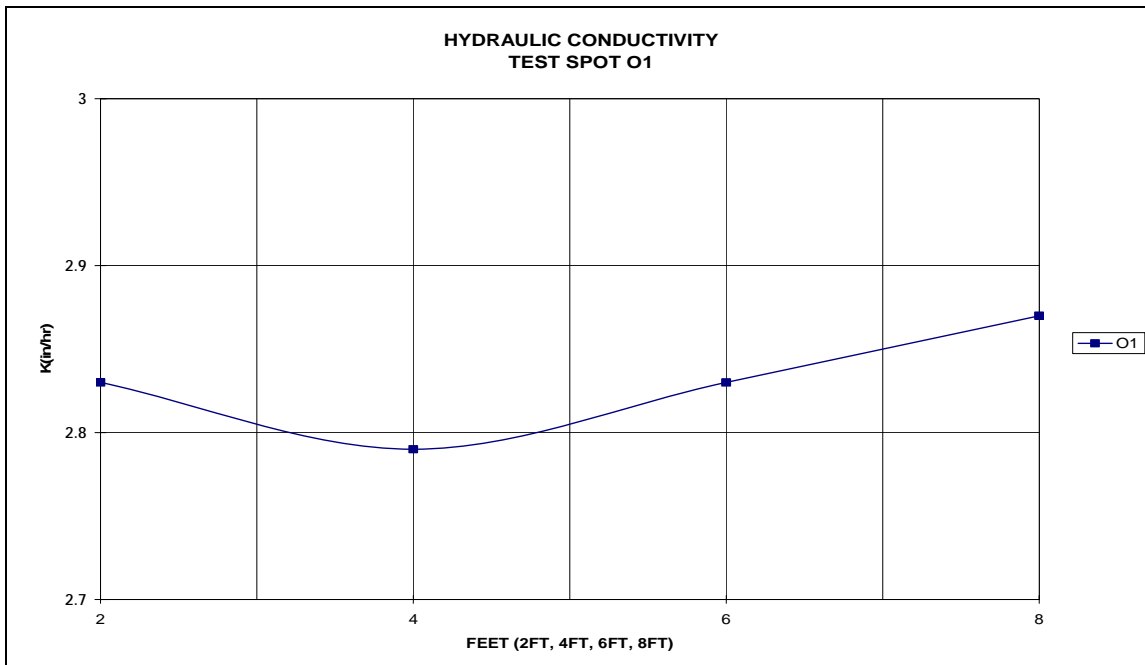


Figure 4.15 – Hydraulic Conductivity Plot of O1

4.7 Total Carbon in Soil Profile and Sediment Load

Figure 4.16 is a graph of total organic carbon at each layer for test locations S1, S2, S3, S4 and SED. L1 was analyzed for total organic carbon. S1 and S2 had the highest values of total organic carbon (TOC) compared to the other three test locations. SED had the lowest content, with S3 and S4 having similar low organic carbon contents. Although S1 had higher TOC values from 0 to 2 inches from the surface, both S1 and S2 had similar readings at lower depths. From a layer and depth point of view, L1 to L3 or 0 to 4 inches from the surface had the highest values in TOC in all five samples. From 4 to 12 inches, the TOC content was steadily maintained at values below 1 percent.

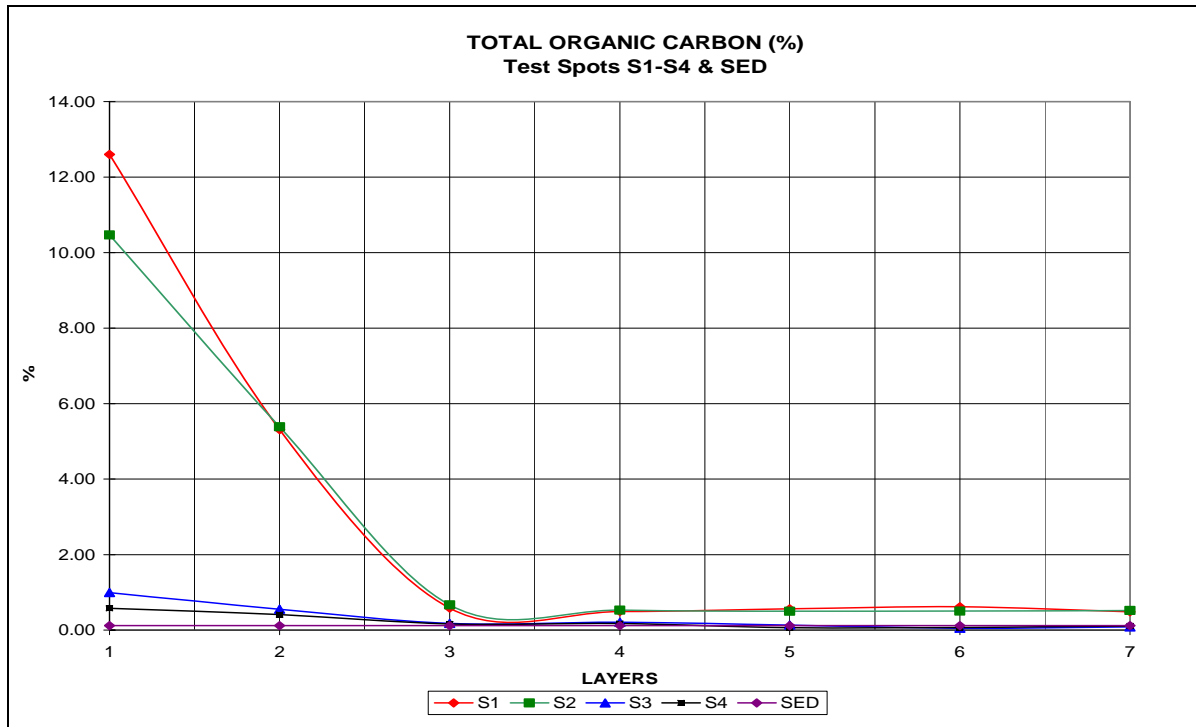


Figure 4.16- Total Carbon Percent Weight for S1-S4 & SED (% by mass)

4.8 Total Nitrogen in the Soil Profile and Sediment Load

Figure 4.17 is a graph of total nitrogen readings for S1 through S4 and SED for all layers. S3 had the highest nitrogen content compared to the other four test locations. S2 had the overall lowest level of nitrogen. However, there is a distinct decrease in all five test locations in terms of layers. Similar to the TOC samples, nitrogen levels sharply decreases from L1 to L3, and then maintained a constant level from L4 onwards.

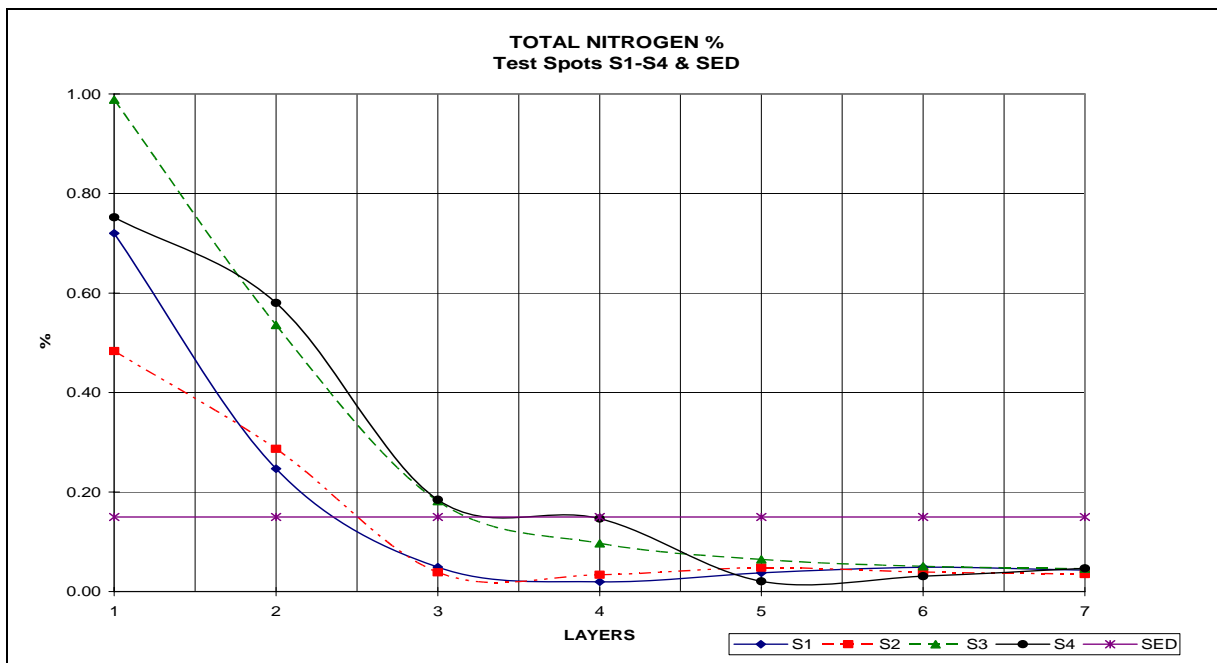


Figure 4.17 - Total Nitrogen Percent Weight for S1-S4 & SED

Chapter Five – Discussion

5.1 Introduction

The basis of this research is to describe any overall changes in the soil profile from time of construction to its current state. Soil moisture content, particle distribution, hydraulic conductivity as well as organic matter distribution are discussed. An analysis of the results obtained is provided.

5.2 Organic Matter Distribution: Carbon and Nitrogen

Soil moisture and organic matter content maintained a similar relationship in terms of depth along the soil profile. Organic matter, carbon, and nitrogen showed a sharp decrease at lower depths. This pattern was found in the soil moisture plot as well. As described in Chapter Two, Stevenson (1982) found that, soil moisture content is be elevated in areas with high organic content. Comparing the two graphs in Figure 5.0, there is a decrease then a constant reading for soil moisture and carbon content from L3 onwards.

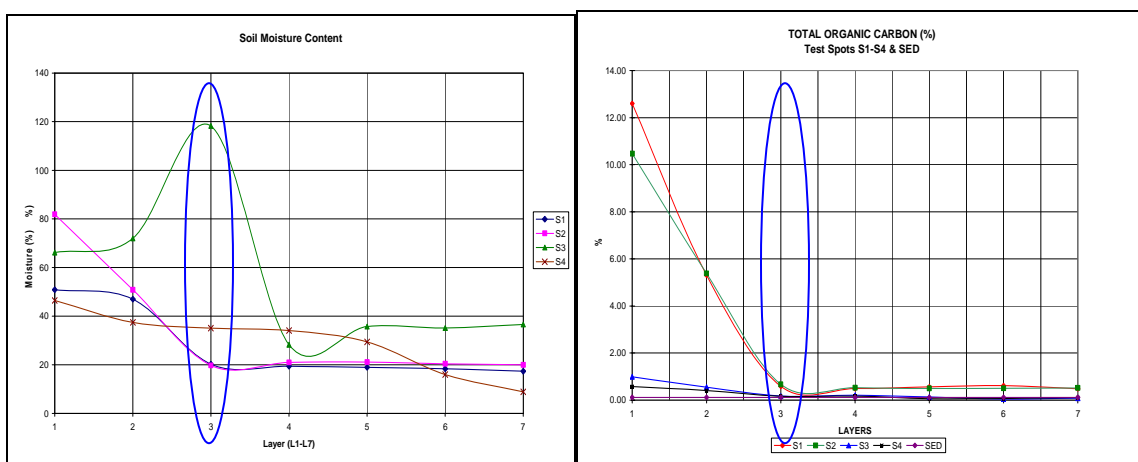


Figure 5.0 – Comparison of Soil Moisture and TOC for S1-S4 and SED

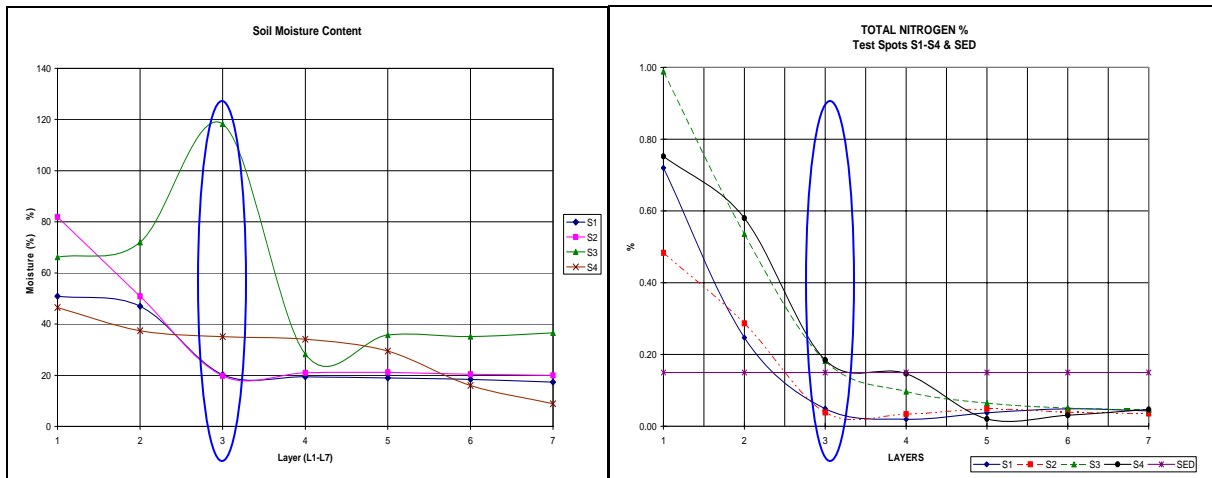


Figure 5.1 – Comparison of Soil Moisture and Total N for S1-S4 and SED

The same relationship is seen when comparing the plots of nitrogen content and soil moisture relationship (Fig 5.1). L3, or 4 inches below the surface signifies an area with high organic matter supporting higher moisture, total carbon and nitrogen. Because this pattern is consistently illustrated in other plots, one may conclude that the basin has an overall 4 inch accumulation of organic matter. This also suggests that the containment of any organic nutrients, either carbon or nitrogen based, seems to be contained within this top 4 inches of soil.

5.3 Fine Content & Soil Distribution – 1ft Profile & 8ft. Profile in Basin

The average percentage of fines in the basin for all test locations along the 1 ft soil profile is 37 percent. Compared to sample SED, with of 48 percent fines, the amount of fine particles for the 1 ft basin samples are less than those deposited from the drainage area. Clay particles contributed 20 to 25 percent of the 37 percent of fine particles present; which classifies soils as sandy loam to sandy clay loam according to the USDA classification system. In the case of S1, the three lowest depths studied (L7, L6 and L5) had an exceptionally high percentage of fines which may suggest some stratification in terms of particle size (Fig. 5.2). However, this was only apparent in S1, which represents the area of lowest elevation and more frequent traction.

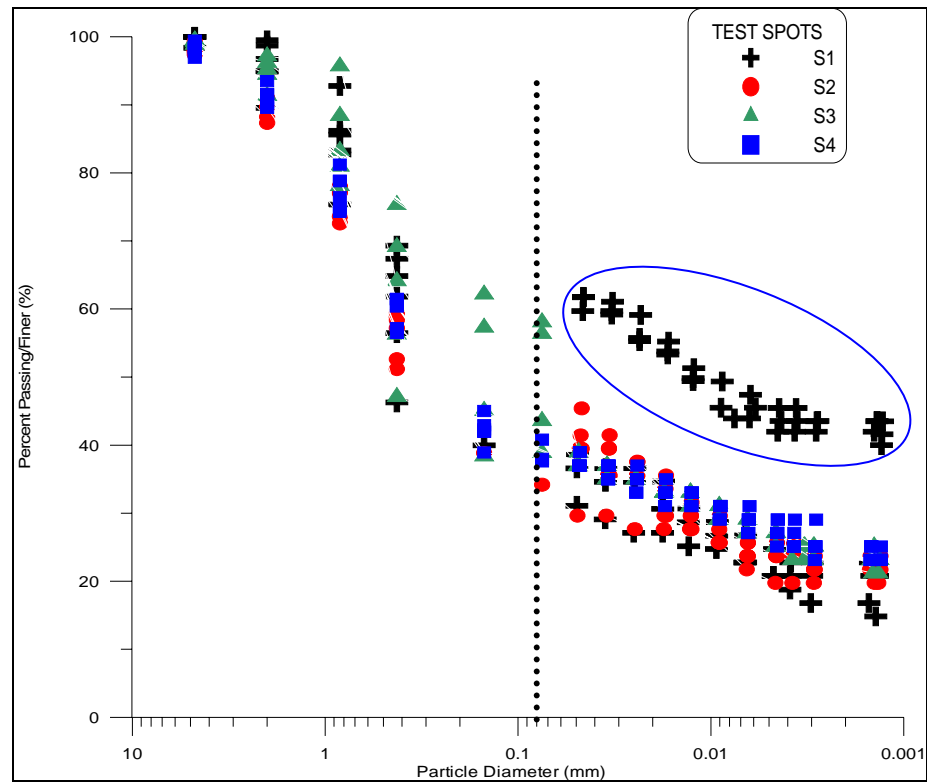


Figure 5.2 – Overall Soil Distribution in Basin S1-S4: High Percent Finer Readings for S1

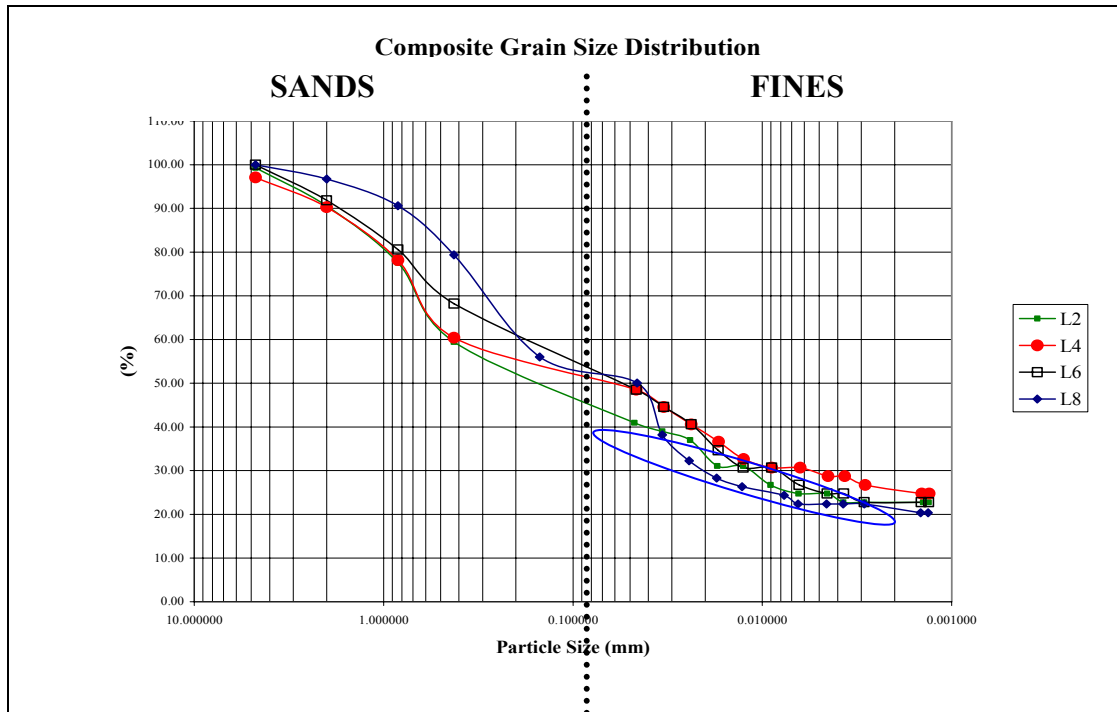


Figure 5.3 – Grain Size Distribution for Eight Foot Soil Profile O1

Comparing individual particle distribution curves for each test location reveals a pattern with soil depth. While the magnitude of variation is small, changes in fine particle content and soil distribution was apparent. In S1 this was most evident because of the possibility of stratification in the upper limits of the profile. This observation suggests that silt and clay particles are gradually increasing at lower depths along the upper 1 ft soil profile.

The 8 ft soil profile study was by far a better measure for the distribution of the soil particles in the profile as it covered the entire 4 ft depth of the designed soil profile and an additional 4 ft beyond into the original soil. L8, at the lowest depth of 8 ft had the lowest percentage of fines (Fig 5.3) compared to the other sampled depths (Table 5.0). L2's soil distribution and fine particle content was similar to that L8. This does not support the suggested relationship of increased fines at lower depths, but shows variation in soil grain distribution. The average percentage of fines is 36 percent, showing comparable values to the studied 1 ft profile.

Percent Passing		Made Soil		Original Soil	
Sieve	Dia (mm)	2 (%)	4 (%)	6 (%)	8 (%)
4	4.750	99.26	97.04	100.00	100.00
10	2.000	90.57	90.26	91.86	96.74
20	0.840	77.55	78.16	80.57	90.58
40	0.425	59.46	60.41	68.21	79.37
100	0.150	40.68	42.95	50.10	56.02
200	0.075	33.60	37.55	38.10	34.73

Table 5.0 – Table Showing Fine Particle Content

5.4 Hydraulic Conductivity – 1 ft and 8 ft Profile in Basin

Theory suggests that particle size distribution, especially fine content of soils determines hydraulic conductivity and suction. The results of the particle analyses show either a decrease, or a constant value for percentage of fines within the 1 ft soil profile from depths L2 to L7. Comparing the particle size distribution shown in Table 5.0 to the hydraulic conductivities in Table 5.1, there is a decrease from the surface to lower depths for most test locations. Although the degree of change is not large, samples like S1 show a significant decrease in hydraulic conductivity from the surface to lower depths. The percentage of fines for S2 fluctuated from surface to lower depths of L5 to L7. However, the overall pattern here suggests no clear relationship between hydraulic conductivity and fine particle distribution.

Layer	Hydraulic Conductivity (in/hr)			
	S1	S2	S3	S4
2	2.75	2.83	--	2.21
3	2.85	2.87	2.81	2.18
4	2.75	2.83	2.77	2.21
5	2.38	2.96	2.77	2.11
6	2.34	2.98	2.77	2.11
7	2.32	2.87	2.77	2.11

Table 5.1 – Tabular Results for Hydraulic Conductivity for S1-S4

Depth	Hydraulic Conductivity (in/hr)
2	2.83
4	2.79
6	2.83
8	2.87

Table 5.2 – Tabular Results for Hydraulic Conductivity for 01

The results of the 8 ft profile shows soil property changes from the designed soil to the original soil beneath. Soil analyses of the 8 ft soil profile show (a) a varied overall particle distribution of soil particles and (b) a sequential particle distribution of total fine particle values from the surface to lower depths. However the calculated results for hydraulic conductivity using

the Sauerbrei formula (Table 5.2) shows a closer relationship with the overall particle distribution illustrated in Figure 5.3. The results vary with a decrease at the 4 ft depth and a gradual increase from 4 to 8 feet. However the decrease at the 4 ft depth reflects the lowest hydraulic conductivity at the bottom of the designed soil profile. Although the magnitude of the change in conductivity is not large, it does suggest varying soil properties at the lowest depth of the designed soil media compared to other depths in the 8 ft profile.

5.5 Original Soil vs. Current Soil Profiles

5.5.1 Comparison of Designed Soil Bed & 8 ft. Soil Profile Samples (Fine Particle Content)

The original grain size distribution data of this site consists of (a) a sieve analysis of the existing soil and (b) an calculated assumption of the sieve analysis for the designed soil profile. Table 5.3 represents the sieve results for the original soil and Table 5.4 illustrates the sieve results for the design soil. The percent passing values for fine soils ($>0.075\text{mm}$) is almost half that of the existing soil which meets its design condition of half the original soil. In Chapter Four, the complete distribution curve of sample B2 is used to further examine the existing soil properties. However, to compare soil properties of the designed soil media in its early stages with its current state; percent finer values passing the No.200 sieve ($>0.075\text{mm}$) is contrasted with the 8ft. profile values. (Fig 5.4)

Dia (mm)	Sieve	Percent Passing
4.7500	4	97.43
2.0000	10	93.06
0.8400	20	86.12
0.4250	40	78.95
0.1500	100	66.26
0.0750	200	58.12

Table 5.3 – Original Soil Sieve Results

Dia (mm)	Sieve	% passing
4.7500	4	96.9
2.0000	10	88.8
0.8400	20	73.17
0.4250	40	53.23
0.1500	100	33.81
0.0750	200	29.15

Table 5.4 – Designed Soil Sieve Results

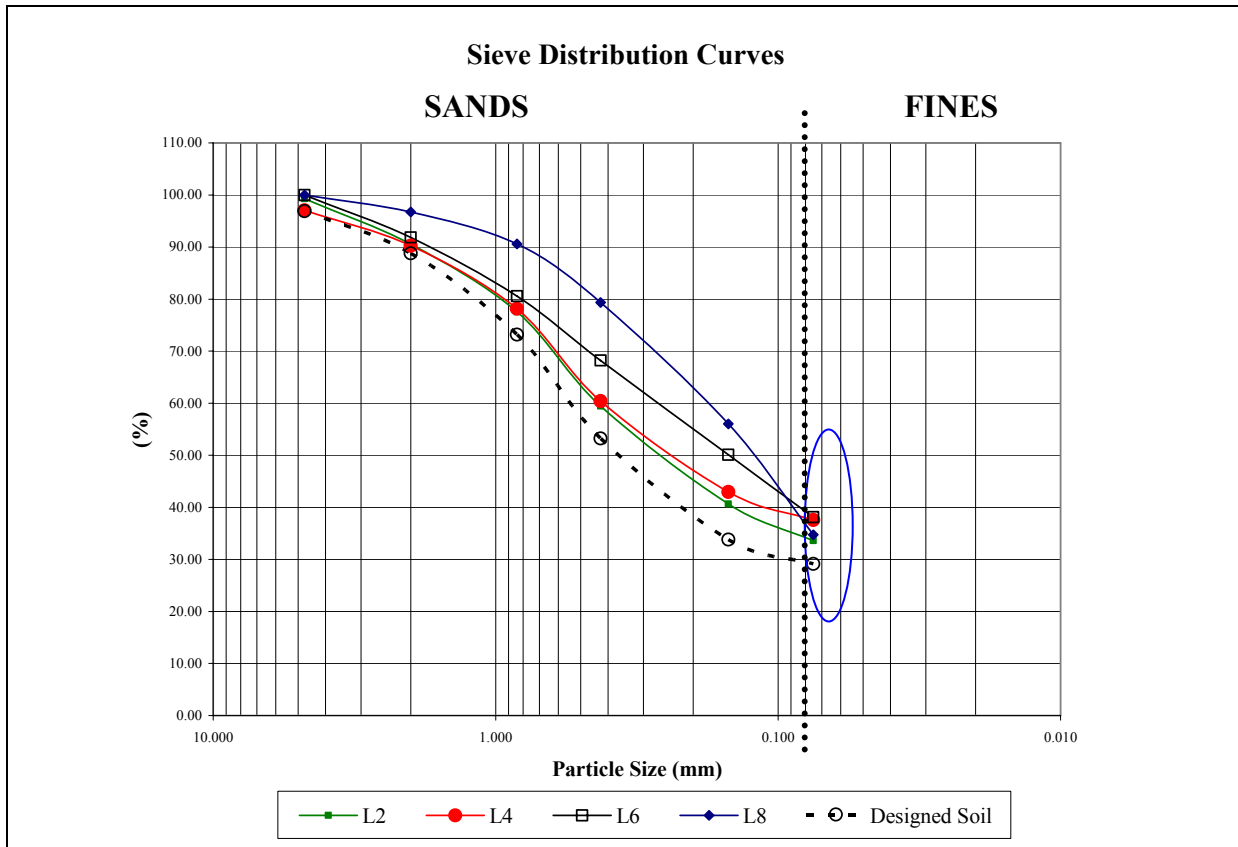


Figure 5.4 – Sieve Test Results for O1 vs Early Designed Soil: Percent Passing No. 200

The plot shows a change in the original designed soil sieve results with each sample layer in O1. L2 was most comparable to the designed soil results at 34 percent finer. L4 and L6 had the highest percentage of fines at 37.6 and 38 percent, respectively. Although a complete distribution is not available for the designed soil, the percentage of fines still shows that variance exists in the original soil properties to the soil currently present at the site. The sand particle distribution from the plot looks comparable although the fine particle content varies. This can only support that the soil properties of the current soil profile is influenced by fine particles containing silt and clay grains.

5.5.2 Comparison of Berm Sample & 8 ft. Soil Profile Samples (Soil Particle Distribution)

The previous section considered the original data retrieved during the construction phase of the project. Because the data was incomplete, the sample B2 representing the berm sample to the right of the outlet will be considered in this comparison with the 8 ft soil profile. B2 is designated as the most comparable sample representing the existing soil on site.

The soil particle distribution of the 8 ft soil profile layers have similar patterns to the B2 sample, which is located on the berm of the basin. L4 is the most comparable layer of the four studied layers. This relationship proves similar characteristics among the existing soil of the drainage area (B2) and the L4 sample. Although the percent passing of each particle (sand, silt and clay) is higher in B2, the particle distribution is similar to L4. It is also understandable that the fine content would be higher, and the sand content lower in B2 compared to the four studied layers of 8 ft soil profile. The results of this analysis may illustrate that the soil properties of the basin layers, particularly L4, have similar soil properties to the existing soil of the site.

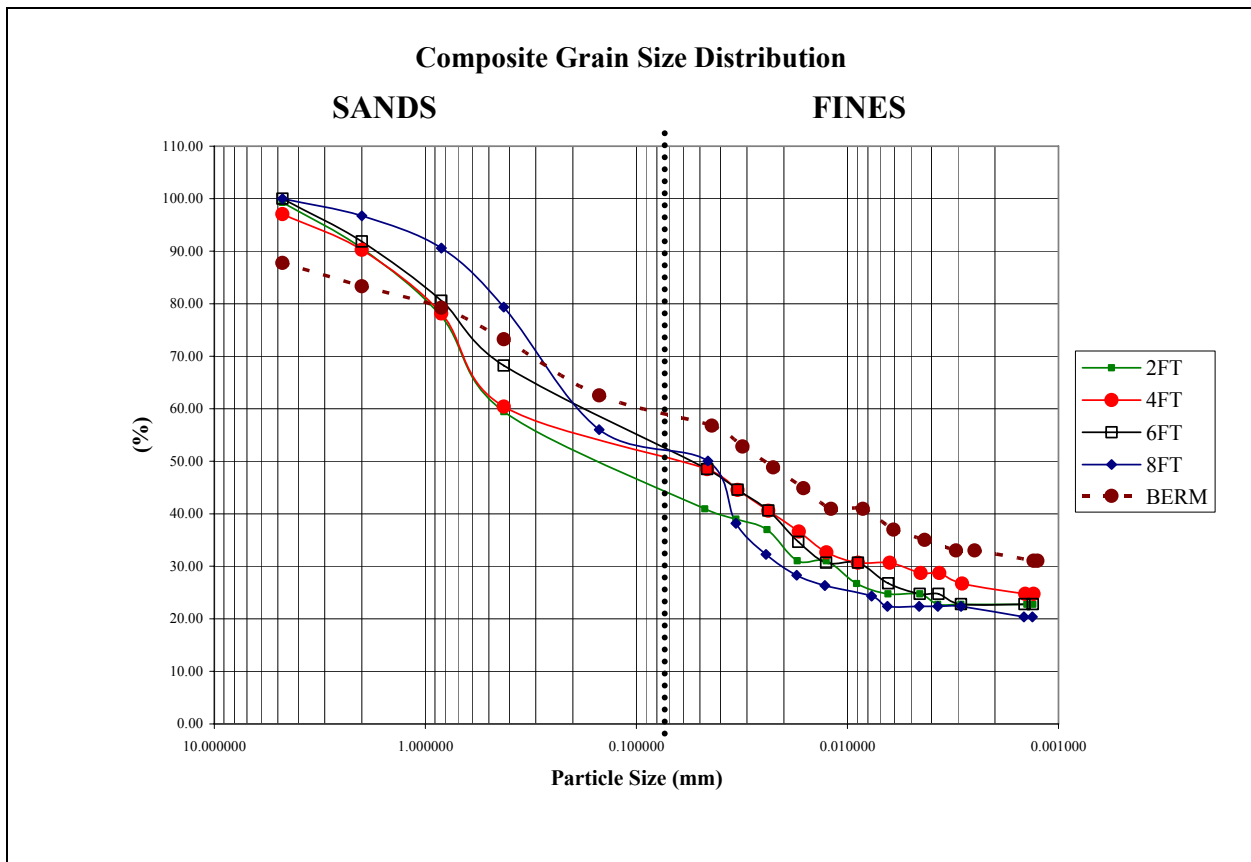


Figure 5.5 – Complete Particle Distribution for B2 vs 8ft Soil Profile

5.6 Possible Sources for Soil Adjustments

5.6.1 Sediment Load

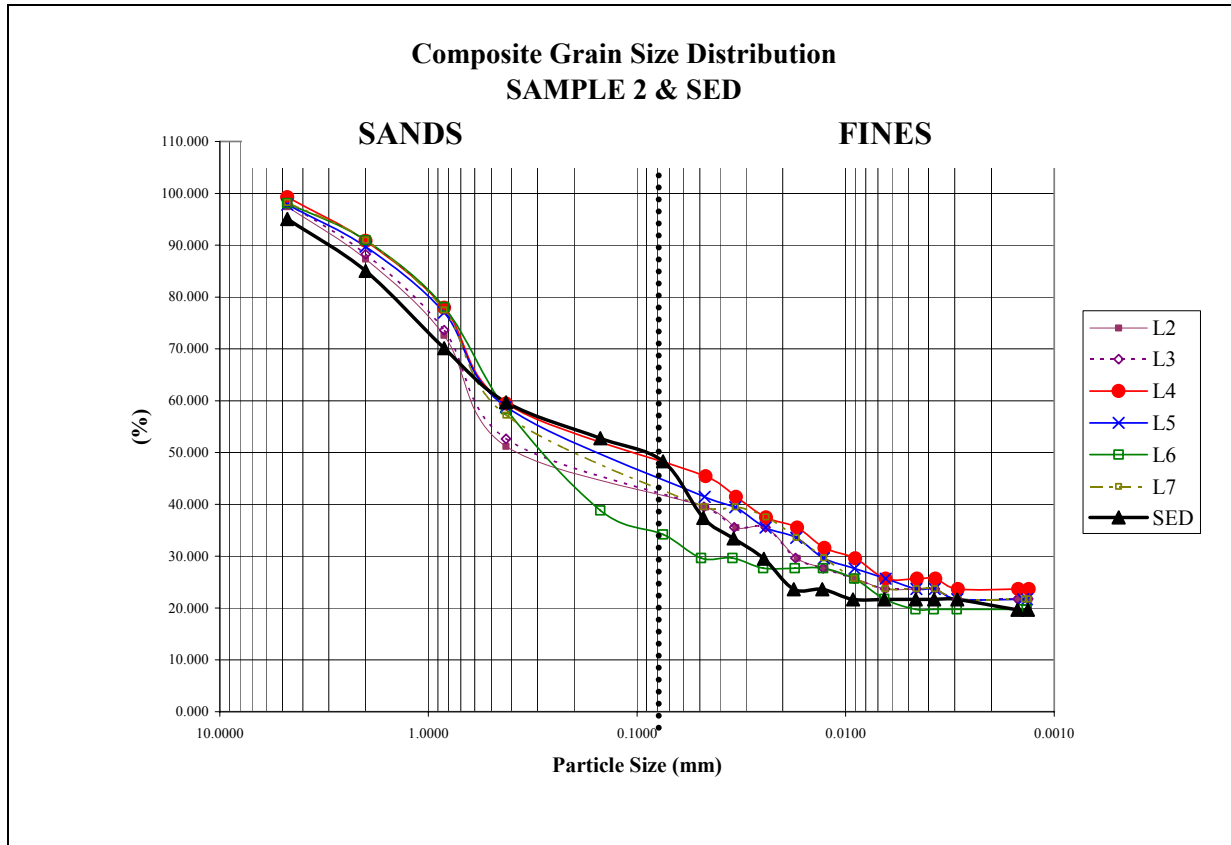


Figure 5.6 – Comparison for Particle Distribution of S2 and SED

<u>S2</u>						
Sieve	L2	L3	L4	L5	L6	L7
4	97.43	98.05	99.28	97.82	98.10	98.21
10	87.35	88.24	90.82	89.73	90.95	90.94
20	72.58	73.58	77.92	77.01	78.07	77.47
40	51.18	52.63	59.44	58.84	58.38	57.20
100	27.23	29.46	38.48	38.32	38.84	37.47
200	23.54	25.77	34.29	33.60	34.19	32.84

<u>SED</u>		
Sieve	Percent Passing (%)	
4	95.05	
10	85.05	
20	70.15	
40	59.69	
100	52.77	
200	48.28	

Table 5.5 – Sieve Results Illustrating Fine Particle Content for S2 & SED

Figure 5.6 and Table 5.5 represent the particle size distribution and of samples S2 and SED. S2 and SED are compared because S2 is located at the foot of the rip rap channel and SED at the mouth of the channel. Although the particle distribution for S2 depicts all layers excluding L6 with similar patterns, the SED sample is non-comparable for silt and clay distribution. The sand distribution is more analogous compared to fines. The total fine content is dissimilar. Samples of S2 have a lower percentage of fines content in all six samples compared to the SED sample. SED had a total fine content of almost 50 percent. These results could reflect two possibilities; (1) the rip rap channel serves to obstruct the flow of sediments to the basin whereby higher fines are present at the mouth of the rip rap channel and (2) only sand particles from the surrounding area may enter the basin during flow events because of relatively similar distribution and sand content. However, the source of sediment in the basin from flow transported from the surrounding drainage area cannot be presumed from this research.

Chapter 6 – Conclusion

6.1 Summary

A relationship exists between organic matter content, consisting of total carbon and nitrogen, and soil moisture content at the Bioinfiltration Traffic Island site. According to Stevenson (1982), depths which have considerable levels of soil moisture content reflect similar levels of organic content as compared to other depths. The depths in this case are nearest to the surface, from zero to 4 inches. It is also within this depth that larger quantities of total carbon and nitrogen are present. At the 4 inch mark, levels of organic matter drop drastically. This signifies capture of these substances at the topmost layer of the soil in the infiltration system. With respect to water quality, this indicates that the soil profile of an infiltration feature is

capable of capturing incoming nutrients and other pollutants. The elevated levels of organic matter also serve to sustain plant life in the basin. The sequestering of possible pollutants within the topmost layer allows easy removal if needed during maintenance practices, as compared to lower depths that may require excavation.

Soil particle distribution controls soil-water properties such as hydraulic conductivity and suction head. Evaluating the basin's performance from the time of construction to its present state requires investigation of soil properties during both stages. The total fine particle content of one and eight foot profiles show small variation along the depths studied. Although the change is small, the general pattern shows increases in silt and clay particles at lower depths for the 1 ft profile. The 8 ft profile does not support this pattern. The soil particle distributions for both profiles are similar and suggest a sandy loam to sandy clay loam soil in the designed soil profile. The only exception for both content and distribution exist in the sample location in the area of lowest elevation and frequent traction, suggesting stratification within the one foot soil profile.

Comparison of the initial and current soil properties of the designed basin was analyzed on the 8 ft soil profile for a broader view of both fine content and soil particle distribution. The soil samples during the initial stage shows a higher percentage of fines compared to the 8 ft soil profile samples. Although small variations exist, it does, however, describe the soil-water properties during both stages in the basin's lifespan. A comparison of the existing soil at the site and the 8 ft soil profile was conducted to evaluate similarities between the two soil samples. Similarities in the two soil samples could support change in the basin's soil properties to reflect that of the existing soil of the site and surrounding drainage area.

This impact would result in a change in the soil's ability to infiltrate water. The results show that while the distribution of fine particles is similar between the two groups of samples, the content of fine particles is smallest in the existing soil sample. The bottom of the designed

profile had the most similar distribution to the existing soil sample, with high fines. It is likely that the base of this profile is creating an interface between the designed profile and original soil beneath. In this case, the soil and its conductivity will differ considerably from the depths above and below. Further research of this 4 ft interface is necessary at various locations within the basin before a general conclusion can be made.

Hydraulic conductivity calculated for all samples reflect similarities with the soil properties with a focus on the content and distribution of fine particles present. Therefore the results show the equivalent small change in value among depths studied. The maximum change among samples is twenty percent. It is safe to say that the overall hydraulic conductivity can be considered constant at averages of 2.81 in/hr and 2.60 in/hr for the 4 ft profile and 1 ft profile, respectively. While soil content and distribution varies in the basin at various locations, the magnitude of change is insignificant to alter hydraulic conductivity at various depths. It is important to note that the terms hydraulic conductivity and infiltration are related, but not the same. Hydraulic conductivity is a function infiltration; therefore other factors not measured in this study are responsible for the overall infiltration rate at this site.

Investigating any changes in the soil profile from its initial stages means studying possible sources that will contribute to the soil adjustment. A comparison of sediment found at the mouth of the rip rap channel and the test location S2, which is located at the foot of the channel, were evaluated for sediment flow into the basin. Results show that the percentage of fines in the sediment load is considerably higher than those found in samples of S2, and other samples at test locations in the basin. While a significant amount of this sediment is always present near the mouth of the channel during storms, the soil analyses does not show any large deposits of fine sediment soil near S2 or surrounding areas. This finding supports the use of rip

rap channels as a pre-treatment in stormwater management systems for reducing incoming sediment and other fine soils from the drainage area.

In conclusion, the current soil profile Bioinfiltration Traffic Island is slightly different than its initial designed composition after 7 years. However, the extent of these differences are minute and do not alter the overall soil-water characteristics of the soil profile. The use of pre-treatment systems, such as rip rap channels and grassed swales, reduce the amount of sediment entering the infiltration system. However, maintenance of these pre-treatment systems is important to reduce excessive sedimentation. The high capture levels of organic materials and soil moisture within the topmost depths of the soil profile shows the capability of bioinfiltration systems in water quality enhancement and plant preservation. Further studies should be carried out to evaluate the capture of other nutrients and pollutants in the topmost depths of the soil profile.

6.2 Design & Maintenance Recommendations

Change in the soil bed from its original composition to its current state, proves the dynamics of soil particles in the presence of water and larger void spaces. While the use of sand soils allowed the existing soil to become more conductive initially, research shows that after several years of performance the conductivity is reducing. Allowing water to travel vertically through the soil profile causes finer particles to move with the flow of water; while building up at the interface where the soil bed meets the subsurface existing soil. The result of this produces varying degrees of change in conductivity along the soil profile. It can be suggested that a soil bed design using the existing soil with the addition of compost on the top layer for plant growth be used. The properties of the existing soil at this site can promote sufficient infiltration without the addition of sand soils. In all cases, the initial design of infiltration features should always

account for the use of the existing soil where conditions are fair. The addition of mulch and compost material within the topmost layers of the soil can also improve its conductivity. The Pennsylvania Department of Environmental Protection recommends infiltration in soils with rates of 0.1 to 10 inches per hour. In situations where the existing soil is not recommended for infiltration careful design of the infiltration bed must occur.

The 4 ft. soil bed was created to incorporate sandy soils into the existing soil at the site, to improve infiltration. This occurred by adding more void spaces into the existing soil through the use of sand particles. While research has shown that infiltration rates at the site were fairly consistent after construction, the physical disposition of the soil profile has changed significantly. With fine particles accumulating at lower depths and large coarse particles nearest to the surface, the design of a soil bed of mixed soil particle defeats its main purpose. The reorganization of these soil particles in the profile will only steadily influence its hydraulic conductivity and other factors controlling the infiltration rate. Therefore the use of a infiltration or seepage beds in the design of infiltration features should account for changes in the overall infiltration rate if beds are constructed using mixed soil particles. However, the same may occur with basins comprising of single sized particles such as sand or rock beds. The contrast between the bed's uniform soil and the existing subsurface soil can create an interface that will impede downward flow. The depth of soil beds may play an important role in hindering changes to infiltration. Deeper designed beds can prolong the intended infiltration rate over a period of time compared to a shallow designed bed, but may still be faced with the challenges created by the interface between the two soil types.

The rate at which the soil profile changes from its initial conditions is highly dependent on the use of pretreatment systems. The use of rip rap channels and grassed swales used at the Bioinfiltration Traffic Island reduced the level of sedimentation within the infiltration basin.

Pretreatment systems such as sediment forebays, settling pools, and natural rock channels should be encouraged in the design of all infiltration features. These systems will enhance the overall performance and longevity of the infiltration BMP, by reducing the inflow of sediments that may hinder long term infiltration capability. Pretreatment also supports a reduction in peak discharge, as well as a decrease in thermal impact and pollutant transport from the surrounding drainage area. Criteria for these pretreatment systems should be designed for a volume capable of treating the entire first flush.

Maintenance of these pretreatment systems should occur throughout the lifetime of the infiltration BMP. Maintenance practices include sediment removal, replanting of vegetation along channels and stabilization of rock and other materials along channels from erosion. The upkeep of pretreatment systems used with infiltration BMPs reduces the need to maintain the actual soil bed of the basin. Avoiding interference of the soil bed of an infiltration basin will sustain its ability to infiltrate and support water quality improvement characteristics. Research showed that the topmost layer of the basin held suitable soil moisture content and contained high levels of nutrients. Reducing soil bed impacts will provide a media for initial inflow filtration as well as provide suitable conditions for plant growth. The upkeep of vegetation in the basin should be minimized, but not completely eliminated in the operation and maintenance of the infiltration BMP. Controlling the growth of vegetation can maintain its aesthetics as well as reduce excessive quantities of nutrients produced from decaying plant life on the surface of the basin. However, it is important to sustain this vegetation for several factors such as nutrient uptake, thermal reduction and evapotranspiration.

6.3 Future Research

This research can be improved and extended through further investigation of infiltration BMPs design criteria, drainage area characteristics and the use of pretreatment systems. While

most analyses may require extended periods for the performance of these BMPs, research can be carried out on existing infiltration features with varying parameters. The role of pretreatment systems can be further extended by comparing the performance of varying pretreatment methods on the reduction of inflow sedimentation. The characteristics of the drainage area are also important and should be investigated with varying levels of sedimentation and nutrients entering the basin. It is important to analyze the performance of the infiltration system with high loading rates from the drainage area.

Research can be conducted simultaneously with several prototypes replicating various design criteria, drainage area characteristics and pretreatment methods. An annual account of the changes in sedimentation within the basin as well as nutrient capture in the topmost layer, can give a better understanding on infiltration longevity. Soil, chemical and moisture analyses performed in this research can occur on an annual or bi-annual basis for all infiltration features constructed. However, disturbance must remain minimal to promote continuous performance. A collection of data over a period of years can clearly identify the changes in the profile. Pretreatment features must also be monitored for their removal of sediments and fine particles in the basin's inflow. It is important to uphold consistency in maintenance and vegetation harvest at each site. The impact of vegetation harvest has influence on the outcome of nutrient capture in the topmost layer of the soil bed. Maintenance of the basin and pretreatment systems can control sediment loading and basin sedimentation.

References

Alyamani, M. S. and Z. Sen (1993). "Determination of Hydraulic Conductivity from Complete Grain Size Distribution Curves." *Ground Water* 31(4): 551-555.

Bodman, G. B. and E. A. Colman (1965). "Moisture and energy conditions during downward entry of water into soils." *Soil Science Society of America Proc* 8: 116-122.

Coduto, D. P. (1999). *Geotechnical Engineering- Principles and Practices*. Upper Saddle River, Prentice-Hall, Inc.

Edwards, W. M. and W. E. Larson (1970). "Infiltration of water into soils as influenced by surface seal development" *Trans. ASAE* Volume 12: 463-465, 470.

Fredlund, M. D., D. G. Fredlund (1997). *Prediction of the Soil-Water Characteristic Curve from the Grain-Size Distribution and Volume-Mass Properties*. 3rd Brazilian Symposium on Unsaturated Soils, Rio de Janeiro, Brazil.

Hanks, R. J. and S. A. Bowers (1962). "Numerical solution of the moisture flow equation for infiltration into layered soils." *Soil Science Society American Journal* Volume 26: 530-534.

Heasom, W., R. Traver and A. Welker (2006). "Hydrologic Modeling of a Bioinfiltration Best Management Practice." *Journal of the American Water Resources Association* Volume 42(No 5): 1329-1347.

Hillel, D. (1998). *Environmental Soil Physics*. San Diego, Academic Press.

Kasenow, M. (2002). *Determination of Hydraulic Conductivity From Grain Size Analysis*. Denver, Water Resources Publications, LLC.

Miller, D. E. and W. H. Gardener (1962). "Water infiltration into stratified soil." *Soil Science Society of America Proceedings* Volume 26: 115-118.

Mohanty, B. P., R. S. Kanwar (1994). "Comparison of Saturated Hydraulic Conductivity Measurement Methods for a Glacial-Till Soil." *Soil Science Society of America Journal* Volume 58 (No. 3): 672-677.

Morrill, L. G., B. C. Mahilum (1982). Organic Compounds in Soil: Sorption, Degradation and Persistence. Ann Arbor, Ann Arbor Science Publishers.

NRC (1993). Soil and Water Quality - An Agenda for Agriculture. *N. A. o. Sciences*, National Academy Press.

PADEP (2006). *Pennsylvania Best Management Practices Manual*.

Pitt, R., J. Lantrip (1999). Infiltration Through Disturbed Urban Soils and Compost-Amended Soil Effects on Runoff Quality and Quantity
Research Report. *U. S. E. P. Agency*, Office of Research and Development.

Prokop, M. (2003). Determining the Effectiveness of the Villanova Bio-Infiltration Traffic Island in Infiltrating Annual Runoff. *Department of Civil and Environmental Engineering. Villanova, Villanova University*. Master of Civil Engineering.

Simka, D. E. (1983). "Soil water change as related to position of wheat straw mulch on the soil surface." *Soil Science Society American Journal* Volume 47: 988-991.

Skaggs, T. H., L. M. Arya (2001). "Estimating Particle Size Distribution from Limited Soil Texture Data." *Soil Science Society of America* Volume 65: 1038-1044.

Smith, R. E. (1990). "Analysis of infiltration through a two-layer soil profile." *Soil Science Society American Journal* Volume 54: 1219–1227.

Stevenson, F. J. (1982). *Humus Chemistry: Genesis, Composition, Reactions*. New York, John Wiley and Sons.

Tate, R. L. (1987). *Soil Organic Matter - Biological and Ecological Effects*. Canada, John Wiley & Sons.

Vukovic, M. and A. Soro (1992). *Determination of Hydraulic Conductivity of Porous Media from Grain Size Composition*. Littleton, Water Resources Publications.

Winegardner, D. (1995). *An Introduction to Soils for Environmental Professionals*, CRC.